Astronomy & Astrophysics manuscript no. main
September 1, 2025

Catalogue of central stars of extragalactic planetary nebulae

W. A. Weidmann[1,2], M. B. Mari[1,2], R. A. Pignata[1,2], M. M. Miller Bertolami[2,3], E. O. Schmidt[1,2,5], and K. Werner[4]

[1] Universidad Nacional de Córdoba, Observatorio Astronómico de Córdoba, Laprida 854, X5000BGR Córdoba, Argentina
e-mail: walter.weidmann@unc.edu.ar
[2] Consejo Nacional de Investigaciones Científicas y Técnicas (CONICET), Godoy Cruz 2290, CABA, CPC 1425FQB, Argentina
[3] Instituto de Astrofísica de La Plata, Consejo Nacional de Investigaciones Científicas y Técnicas Avenida Centenario (Paseo del Bosque) S/N, B1900FWA La Plata, Argentina
[4] Institut für Astronomie und Astrophysik, Kepler Center for Astro and Particle Physics, Eberhard Karls Universität, Sand 1, 72076 Tübingen, Germany
[5] Instituto de Astronomía Teórica y Experimental (IATE, CONICET-UNC), Laprida 854, X5000, Córdoba, Argentina

ABSTRACT

Context. Central stars of planetary nebulae (CSPNe) are essential for understanding the final evolutionary stages of low- and intermediate-mass stars. However, their study in extragalactic environments remains challenging due to their intrinsic faintness and the limited availability of high-quality data.

Aims. We aim to provide a comprehensive and up-to-date catalogue of extragalactic CSPNe in order to enable a more complete view of their physical properties across different galactic environments and metallicities.

Methods. The catalogue was assembled using data from the most recent and reliable literature sources. Priority was given to collecting effective temperatures and luminosities that have either been directly reported or consistently derived. When available, spectral types or specific spectral features – such as P-Cygni profiles or broad Hα emission lines – were also included. This approach allowed for broader characterisation of the sample, even when accurate classifications are not available.

Results. We present a new compilation of extragalactic CSPNe – the largest to date – comprising over 800 objects located in the Magellanic Clouds, NGC 300, NGC 5128, and fifteen other nearby galaxies. This catalogue enables, for the first time, a global comparison of CSPNe physical parameters beyond the Milky Way. Updated Hertzsprung–Russell diagrams are provided featuring CSPNe from seven different galaxies, revealing trends and outliers that merit further investigation. The catalogue represents a valuable resource for future spectroscopic follow-up and for improving our understanding of post-AGB evolution in diverse galactic contexts.

Key words. Catalogs – planetary nebulae: general – stars: evolution – Local Group

1. Introduction

Planetary nebulae (PNe) represent a brief phase in the evolution of low- and intermediate-mass stars, i.e. those with masses between 0.8 and 8.0 M$_\odot$. Within the standard single stellar evolution scenario, PNe are formed when the progenitor star ejects most of its envelope and the remaining stellar remnant contracts and heats up. During this stage, the previously ejected material is ionised by the central star, producing the characteristic glowing structure (Kwok 2007; Kwitter & Henry 2022). The central stars of planetary nebulae (CSPNe) play a fundamental role in shaping the morphology and evolution of PNe. Additionally, they serve as valuable probes of stellar evolution, providing insight into the properties of stellar populations and the chemical composition of their host environments.

In the Milky Way (MW), extensive efforts have been made to catalogue PNe and their central stars. A key contribution to the latter is the compilation by Weidmann & Gamen (2011); Weidmann et al. (2020); González-Santamaría et al. (2021), which made it possible to assess the detectability of CSPNe. That catalogue showed that only about ∼21% of CSPNe can be identified and characterised in terms of their properties, such as temperature and luminosity, due to observational challenges and intrinsic faintness. Additionally, Weidmann et al. (2020) found that 50% of the sample (88 out of 175 objects) with derived values of luminosity (L), effective temperature (T_{eff}), and surface gravity (g) have masses and ages consistent with single stellar evolution models, suggesting that some single stars are indeed capable of forming PNe.

Due to their brightness, PNe can be detected in other galaxies. Notably, Jacoby (1989) and Ciardullo et al. (1989) demostrated that PNe can serve as distance calibrators through the planetary nebula luminosity function (PNLF). Significant efforts have been devoted to identifying PNe in other galaxies, leading to the discovery of several thousand extragalactic PNe (e.g. Ford et al. 2002; Magrini 2006). Moreover, intracluster PNe have even been detected (e.g. Arnaboldi et al. 2007; Spiniello et al. 2018).

The study of PNe in extragalactic environments offers a complementary perspective to that of the MW, helping to clarify how factors such as metallicity and star formation history influence stellar evolution (Jacoby & Ciardullo 1999; Stanghellini & Haywood 2010; Valenzuela et al. 2025). Extragalactic PNe have been identified in galaxies such as the Magellanic Clouds (Reid & Parker 2010a), M 31 (Merrett et al. 2006), and M 33 (Ciardullo et al. 2004), providing unique data on stellar evolution across different galactic environments. However, characterising the extragalactic CSPNe is more challenging due to their low luminosity and the distances involved (Gesicki et al. 2018).

Despite these challenges, the growing amount of published data opens the possibility of consolidating existing information into a unified catalogue. Previous efforts, such as the most recent catalogue of CSPNe by Weidmann et al. (2020), have demonstrated the value of systematic data collection in enabling robust statistical and comparative studies.

In this work, we present a compilation of inferred properties of extragalactic CSPNe. In particular, we focus on their T_{eff}, L, and (when available) their spectral type (SpT). While the spectral type provides essential information about the evolutionary status of these stars, obtaining it is particularly challenging due to the low brightness of the targets. As a result, the properties of a significant part of these central stars – such as L, T_{eff}, and even spectral classification – have been inferred through modelling efforts rather than direct observations. This catalogue integrates data from direct measurements and models, offering a valuable resource for investigating how the properties of central stars vary across different galactic environments. We expect this catalogue to serve as a foundation for future observational and theoretical studies on stellar evolution across diverse environments.

While the primary objective of this work is to provide a comprehensive compilation of candidate CSPNe, we acknowledge that not all objects included can be considered confirmed PNe. Similarly, the derived or compiled stellar parameters (e.g. effective temperature and luminosity) should be treated with caution. Given the limitations and heterogeneity of the available data, we emphasise that this catalogue is intended as a resource for exploratory analysis and future observational follow-up, rather than as a definitive dataset for deriving robust correlations with metallicity or progenitor mass.

The structure of this paper is as follows. In Section 2 we provide a detailed description of the catalogue and discuss its limitations, while in Section 3 we analyse and discuss the distribution of the physical parameters of the extragalactic PNe. Finally, the discussion and conclusions are presented in Section 4 and 5.

2. The catalogue of extragalactic CSPNe

The main objective of this work is to compile known properties of extragalactic CSPNe, including the spectral type (SpT), $\log(L/L_{\odot})$, and $\log(T_{eff})$. The catalogue includes 1073 objects across 19 galaxies. Table 1 presents the main characteristics of these galaxies. Nearly all the galaxies included, except M 81, NGC 5128, NGC 300, and NGC 5236, are members of the Local Group. This underscores the substantial volume of extragalactic PNe with available spectroscopic data.

While the catalogue provides a comprehensive list of CSPNe, only a few of the entries include references to spectral type, with the majority of these objects located in the Large Magellanic Cloud (LMC).

Data were gathered from refereed publications post 1985. For objects with multiple determinations, we report the most recent values. Information in the catalogue, organised by galaxy and right ascension (RA), includes the following:

- Col. 1: Name of the PN, prioritising the designation used in the original publication from which the data was obtained.
- Col. 2: Host galaxy.
- Col. 3-4: The RA and DEC as listed in the original publications, with minimal differences from the Centre de Données astronomiques de Strasbourg (CDS).
- Col. 5-6: Logarithm of the CSPN's effective temperature ($\log\ T_{eff}$) and its reference. In some galaxies, data for the central star were unavailable. However, the emission line intensities of the PNe that could be identified have been reported in the literature. In these cases, we were able to estimate the temperature (see Sec. 3.3).
- Col. 7-8: Logarithm of the luminosity, in units of solar luminosity ($\log\ L/L_{\odot}$), and reference source. In the same way as for the temperature, we have been able to compute the luminosity using the magnitude of the nebula at [O III]λ5007 (see Sec. 3.3).
- Col. 9-10: Spectral type and reference. In cases where the spectral type was not explicitly listed, additional information (e.g. P-Cygni profiles, broad Hα emission) helped us infer the characteristics.
- Col. 11: References identifying the CSPN as a binary system.
- Col. 12: Comments.

The coordinates have been rounded to the nearest tenth or to '.00' where precision is lacking. We followed the same criterion for $\log(L/L_{\odot})$ and $\log(T_{eff})$. While errors for the physical parameters are sometimes given in the original publications, they are not included in this catalogue. We provide a discussion on uncertainties in Sec. 2.1.

2.1. A few caveats

As mentioned earlier, only a few extragalactic CSPNe have a spectral classification. Detecting an O(H) star is challenging due to their faint absorption lines, which require a high signal-to-noise (S/N) spectra. In contrast, Wolf-Rayet ([WR]) stars are easier to identify even with a lower S/N in the continuum, as their strong emission lines are prominent. Indeed, in this catalogue, the vast majority of CSPNe with a determined spectral type are [WR].

For all reported objects, the parameters of the central star were estimated from the observed nebular spectra. While most properties were primarily inferred using CLOUDY models (Ferland et al. 1998, and references therein), in some cases, the Zanstra temperature was also determined (e.g. Villaver et al. 2004). This limitation directly affects the accuracy of stellar parameter determinations. Moreover, in most cases, only low-quality spectra are available, thus only allowing for an estimation of temperature and luminosity (see Sec. 3.3). The most reliable approach to accurately obtaining physical parameters for CSPNe is through fitting stellar atmosphere models to their spectra (e.g. Mendez et al. 1988). To illustrate the uncertainties associated with the stellar parameters listed in our catalogue, Table 2 presents examples of extragalactic CSPNe with varying determinations of these physical parameters. In addition, in Section 3.5 we present a discussion on the uncertainties associated with two specific methods.

Another crucial aspect to consider is that the objects in this catalogue should be regarded as PN candidates, even if the paper does not explicitly state this. These objects are poorly studied, and in most cases there is only a single spectrum available. Especially considering that PNe are perhaps one of the most difficult objects to classify, their status only as candidates should not be overlooked (Frew & Parker 2010).

Additional considerations must also be addressed. Murset & Nussbaumer (1994) proposed an empirical relationship between the temperature of the ionising source (T_*) in a photoionised gaseous nebula and the highest observed ionisation potential (χ_i):

$$T_* = \chi_i \times 1000 \qquad [K/eV]. \tag{1}$$

In general, extragalactic PNe are identified by means of the interferential filter centred on [O III]λ5007. In this context, the temperatures of the extragalactic CSPNe of our catalogue will be higher than 35100 K.

Table 1. Main parameters of the galaxies in our sample. Namely, these are galaxy name, number of catalogued PNe, metallicity, morphological type, color, and global stellar mass.

Galaxy	# PNe	[Fe/H][(1)] dex	Morph type (NED)[(2)]	$(B\text{-}V)^0_T$ (RC3)[(3)]	$\log(M_g/M_\odot)$
MW	206	-	SBc	-	10.78[(6)]
LMC	121	-0.31 ± 0.04[(7)]	SB(s)m	0.43	9.15[(4)]
SMC	47	-0.97 ± 0.05[(8)]	SB(s)m pec	0.36	8.59[(4)]
M 31	40	-	SA(s)b	0.76	10.95[(4)]
M 32	10	-1.1 ± 0.2	compact E2	0.88	9.07[(4)]
M 33	11	-	SA(s)cd	0.46	9.61[(4)]
M 81	11	-	Sb(r)I-II	-	11.36[(10)]
IC 1613	1	-1.3 ± 0.2	IB(s)m	0.65	8.00[(5)]
NGC 147	6	-1.1 ± 0.2	E5 pec	0.78	8.30[(4)]
NGC 185	1	-1.2 ± 0.15	dE3p	-	7.83[(5)]
NGC 205	4	-0.8 ± 0.1	Sph	-	8.47[(5)]
NGC 300	41	-0.5[(9)]	SA(s)d	0.56	9.41[(4)]
NGC 3109	1	-1.5 ± 0.3	SB(s)m[c]	-	8.18[(4)]
NGC 5128	557	-	S0+S pec	-	-
NGC 5236	2	-	Scd?	0.61	-
Fornax dSph	1	-1.3 ± 0.2	dE4	-	7.30[(5)]
Phoenix	1	-1.9 ± 0.1	lAm	-	5.88[(5)]
Sextans A	1	-1.9 ± 0.3	lBm	0.35	7.64[(5)]
Sextans B	5	~ -1.2	lB(s)m	0.47	7.71[(5)]
Sgr dSph	3	-1.0 ± 0.2	dSph(t)	-	7.32[(5)]

References. (1) Mateo (1998); (2) NASA/IPAC Extragalactic Database; (3) de Vaucouleurs et al. (1991); (4) Delgado-Inglada et al. (2020); (5) McConnachie (2012); (6) Licquia & Newman (2015); (7) Rolleston et al. (2002); (8) Choudhury et al. (2020); (9) Richer et al. (1985); (10) Appleton et al. (1981).

Table 2. Some objects with different determinations in their physical parameters.

PN	$\log T_1$(ref.)	$\log T_2$ (ref.)	$\log T_3$ (ref.)	$\log L_1$ (ref.)	$\log L_2$ (ref.)	$\log L_3$ (ref.)
LMC-SMP 35	5.07 (DM91c)	5.03 (DV97)	4.78 (HB04)	3.17 (DM91c)	3.38 (DV97)	3.01 (HB04)
LMC-SMP 67	4.64 (DM91c)	4.74 (HB04)	4.69 (VS07)	3.33 (DM91c)	3.70 (HB04)	3.40 (VS07)
LMC-SMP 85	4.62 (DM91c)	4.63 (DM91)	4.60 (HB04)	3.85 (DM91c)	3.79 (DM91)	3.41 (HB04)

References. DM91: Dopita & Meatheringham (1991b); DM91c: Dopita & Meatheringham (1991c); DV97: Dopita et al. (1997); HB04: Herald & Bianchi (2004); VS07: Villaver et al. (2007).

Another point to consider is that extragalactic PNe are detected as point sources due to the great distance separating us from them, which prevents their actual extent from being determined and makes it impossible for their surface brightness to be discerned. In this sense, what is actually detected is their integrated brightness. A reasonable assumption that only the brightest PNe are detected. This, in turn, implies that these PNe have bright central stars. Additionally, their nebulae are not too diffuse, making them optically thick and thus favouring their detection. Moreover, according to Ciardullo et al. (2005), the progenitors of the PNe that populate the top 0.5 mag of the PNLF (i.e. the brightest PN) have core masses of $\gtrsim 0.6$ $M_\odot$. Nevertheless, we cannot infer realistic masses with the data currently available and collected in this catalogue. In summary, in the extragalactic context, only the most luminous CSPNe in compact and optically thick nebulae will be detectable.

Finally, given that all the compiled candidate PNe must be relatively bright, it is expected that they are in an early stage of CSPNe evolution. Specifically they are in the flat region of their evolutionary tracks, which is before they begin to lose luminosity as they cool down (see the evolutionary tracks of Miller Bertolami (2016)).

3. Analysis of physical parameters

To compare the distribution of the physical parameters of our CSPN sample with those of the MW, we used the data from the Weidmann et al. (2020) catalogue. The objects that are known to be binary were not considered. Fig. 1 shows the HR diagram, and H-rich and H-poor CSPNe appear to be evenly intermingled. Consequently, in the following figures, no distinction is made between H-rich and H-poor. It is worth noting that the physical parameters of CSPNe in our Galaxy were generally determined using stellar atmosphere models, whereas for extragalactic CSPNe, this method is unfeasible (see Sec. 2.1).

3.1. LMC and SMC

Figure 2 shows $\log(T_{eff})$ versus $\log(L/L_\odot)$ for the LMC and Small Magellanic Cloud (SMC) galaxies along with the sample of CSPNe from the MW previously described. This is the most complete HR diagram of CSPNe to date for these two galaxies. The data for the LMC and SMC were collected from eleven different articles, resulting in variations in the methods used to derive the physical parameters. We note that this may affect the comparison between the different samples in Fig. 2 given

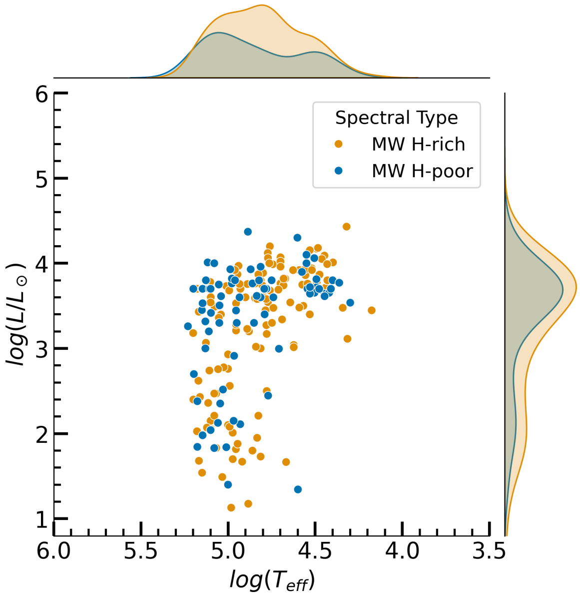

Fig. 1. Hertzsprung–Russell diagram showing CSPNe within the MW from Weidmann et al. (2020). The marginal curves represent the data using a continuous probability density curve.

that the physical parameters were not determined using the same methodologies.

Figure 2 highlights that the point distributions of the LMC and SMC are well mixed. Although the metallicities of the two galaxies (Table 1) are quite different, the quality of the data does not allow us to draw any conclusion about a possible trend with metallicity.

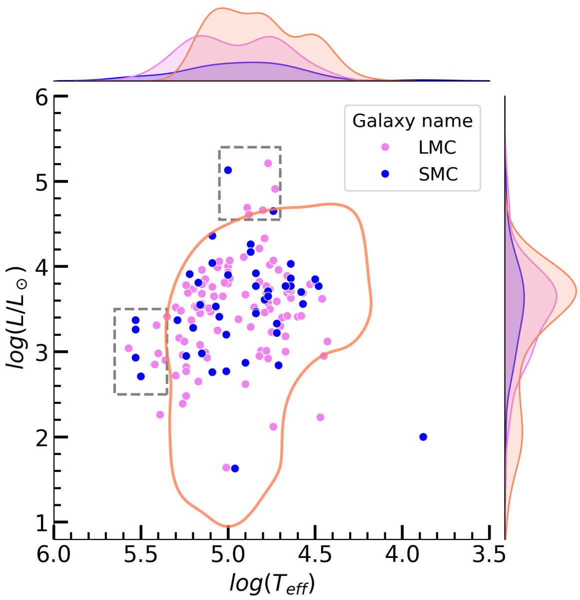

Fig. 2. Hertzsprung–Russell diagram of CSPNe in the LMC and SMC. The coldest CSPN in the SMC likely has poorly constrained parameters, as an effective temperature (T_{eff}) above 10,000 K is required to efficiently ionise hydrogen. The orange contour shows the distribution of points for the MW. In grey, two regions with extreme values are highlighted (see text for details).

Nevertheless, the CSPNe of our most important satellite galaxies occupy the same region of the HR diagram as the CSPNe in our own Galaxy. Although the point cloud of the MW is somewhat shifted towards lower temperatures compared to the points in the LMC and SMC, this is likely attributable to the methodology used for the detection of extragalactic PNe (see comments related to Eq. 1). Additionally, we note that we did not detect PNe with white dwarfs (WD) nuclei. This makes perfect sense, as PNe with WD nuclei are objects with low intrinsic luminosities. Notably, the most luminous CSPNe candidates are found in the Magellanic Clouds (Fig. 2).

In Fig. 2 two regions in the HR diagram that feature high values of temperature and luminosity are indicated. While some objects in these regions are classified as probable PNe or confirmed binaries, others are not. In the high-luminosity region, these sources are unlikely to be CSPNe. According to Miller Bertolami (2016), the most luminous CSPNe reach up to $\log(L/L_{\odot}) \simeq 4.4$, but even in such cases, they would correspond to massive CSPNe with extremely rapid evolution, making them very difficult to detect. Alternatively, these objects might instead be classical WR stars (see Fig. 2 of Shenar 2024).

As for the objects located in the high-temperature region, they could potentially be CSPNe. Incidentally, they would be among the most massive ones. Such a population of very massive CSPNe could be the progeny of high mass stars formed recently (< 1 Gyr) in the Magellanic Clouds (Harris & Zaritsky 2009; Mazzi et al. 2021). Again, such objects evolve quickly, making them difficult to detect. In any case, the sources in this region should be studied in more detail, as we might be looking at a very peculiar CSPN.

3.2. The case of NGC 300

Soemitro et al. (2023) obtained spectroscopic data from a moderate sample of PN in NGC 300. This allowed them to obtain an estimate for the temperature and luminosity of the CSPNe.

The effective temperatures of the CSPNe in NGC 300 were estimated using the empirical excitation class (EC) method defined by Reid & Parker (2010b) as follows:

$$EC_{low} = 0.45 \left[\frac{F(5007)}{F(H\beta)} \right] \tag{2}$$

$$EC_{high} = 5.54 \left[\frac{F(4686)}{F(H\beta)} + \log_{10} \frac{F(4959) + F(5007)}{F(H\beta)} \right], \tag{3}$$

where EC_{low} applies for $0 < EC < 5$ and EC_{high} for $5 \leq EC < 12$. Therefore, the empirical relationship between the excitation class and effective temperature is

$$\log(T_{eff}) = 4.439 + [0.1174(EC)] - [0.00172(EC^2)]. \tag{4}$$

A peculiarity of this temperature estimation method is the discontinuity between Eqs. 2 and 3. As a result, applying it to a large sample of objects may produce an artificial gap in the temperature distribution. It is important to mention that these equations are valid if the nebula is optically thick. In addition, the datasets used did not cover the wavelength range including the He II λ4686 line, which is essential for determining medium- and high-excitation classes. As a result, the effective temperatures (T_{eff}) for excitation classes greater than 5 ($EC \geq 5$) could only be estimated as lower limits, with $\log(T_{eff}) \gtrsim 5$. Conversely, for objects with $EC < 5$, $\log(T_{eff}) < 5$ is expected.

On the other hand, for luminosity estimates, Soemitro et al. (2023) assumed that ~11% of the CSPN's luminosity is efficiently converted into the [O III]λ5007 emission line. This implies that a significant fraction of the CSPN's energy is channeled into this specific line (e.g. Dopita et al. 1992; Schönberner et al. 2010). This assumption is as follows:

$$L_{5007} = 4\pi d^2 F_{5007}, \quad (5)$$

$$L_{5007} = 0.11 L_*. \quad (6)$$

This assumption holds for optically thick nebulae and when [O III]λ5007 is the only coolant. If the nebula is optically thin, the efficiency of this ion decreases, meaning the estimated luminosities represent lower limits, similar to T_{eff}, thus making it difficult to impose stricter constraints on CSPN masses. In this sense, Soemitro et al. (2023) combines Eq. 5 and 6.

The proportionality constant of Eq. 6 depends on factors such as the CSPN mass and the (O/H) abundance (Schönberner et al. 2010) as well as whether it is hydrogen-burning or helium-burning (Jacoby 1989) and the T_{eff} (Dopita et al. 1992).

In summary, as outlined in Soemitro et al. (2023), this represents a lower limit for luminosity and effective temperature. This premise is reflected in the HR diagram of Fig. 3, where many CSPNe fall in the low-L ($log(L/L_{\odot}) < 2.5$) and low-T_{eff} ($log(T_{eff}) < 5.1$) region, where the nebulae have nearly disappeared and only white dwarfs are observed (see Fig. 9 of Weidmann et al. 2020).

3.3. The case of M 81, NGC 185, NGC 3109, and NGC 5128

The emission line intensities of numerous PNe in some well-studied galaxies have been reported in the literature: M 81 (Stanghellini et al. 2010), NGC 185 (Richer & McCall 2008), NGC 3109 (Flores-Durán et al. 2017), and NGC 5128 (Walsh et al. 2015). Using the [O III] and He II lines, we calculated the EC to estimate the effective temperature of the CSPNe, following the method applied by Soemitro et al. (2023), Eq. 2, 3, and 4. This method requires the nebula to be optically thick. To determine if the nebulae is optically thick, we used the criteria as proposed by Soemitro et al. (2023):

$$F(6584)/F(H\alpha) > 0.3. \quad (7)$$

For M 81 and NGC 185, we excluded optically thin objects from our catalogue. Unfortunately, the intensity of the [N II]λ6584 line for objects in NGC 5128 has not been published. In this case, as we do not know the optical depth of the PNe in the sample, we assumed that they are all optically thick. Similarly, although the line intensities of PNe in NGC 3109 have been published (Flores-Durán et al. 2017), these objects were excluded from our catalogue due to their optically thin nature.

As long as the [O III]λ5007 and Hβ lines are visible, the EC can be calculated through both Eq. 2 and 3. To decide which to apply, we adopted the following criterion: If emission from He IIλ4686 is reported, we use Eq. 3; otherwise, we apply Eq. 2. To compute the EC of the PNe in NGC 5128, we used the approximation F(5007) = 3.01 F(4959) (Acker et al. 1989), as the intensity of the 4959Å line is not reported for these PNe.

On the other hand, according to the Eq. 1, a temperature of 54400 K is required to produce He II emission. Moreover, Eq. 4 indicates that an EC greater than ~2.63 is necessary for He II emission. Thus, if Eq. 2 yields an EC lower than 2.6 but He II emission is observed, we attribute this emission to the central star and mark it as "[WR]?".

Three objects in NGC 5128 (namely, P04_4609, EMMI_480, and EMMI_2045) exhibit an EC > 12, which we interpret as indicative of stellar emission. Although these objects are undoubtedly very hot, we did not assign them a specific temperature. Instead, we classified these PNe as [WR] candidates.

Meanwhile, for the identification of extragalactic PNe, images are often captured using interferential filters, particularly those centred on the prominent nebular line of [O III] at 5007Å. This approach is useful for estimating the luminosity of the central stars. It allows for the determination of PN magnitudes in this band (m_{5007}), which can then be used to estimate the central star's luminosity. The integrated monochromatic flux from the [O III]λ5007 (F_{5007}) is related to the m_{5007} magnitude according to the expression given by Jacoby (1989)

$$m_{5007} = -13.74 - 2.5\, log_{10}(F_{5007}), \quad (8)$$

where the flux is expressed in units of $erg\ cm^{-2} s^{-1}$ Å^{-1}.

Equation 8 combined with Eq. 5 and Eq. 6 gives the CSPN luminosity. We used this set of equations to determine the luminosity of CSPN for the PNe in galaxies M 81, NGC 185, and NGC 5128.

As mentioned in Sec 3.2, this method of determining luminosity applies if the nebula is optically thick and that [O III]λ5007 is the only cooling mechanism. For NGC 5128, we assumed that all nebulae in the sample are optically thick.

The magnitudes, m_{5007}, of the PNe in NGC 5128 have been compiled from the ESO Multi Mode Instrument catalogue (EMMI, Walsh et al. 2015) and Hui et al. (1993). For objects with magnitudes available in both works, we applied flux averaging.

We assumed distances of 3.89 Mpc for NGC 5128 (Beasley et al. 2024), 3.63 Mpc for M 81 (Freedman et al. 2001), and 0.616 Mpc for NGC 185 (Geha et al. 2010). Additionally, we adopted a solar luminosity of $L_{\odot} = 3.826\times10^{33} erg\ s^{-1}$ (Ostlie & Carroll 1996). The resulting $\log(L/L_{\odot})$, together with $\log(T_{eff})$ values are presented in our catalogue.

The HR diagram is shown in Fig. 3 along with the values for NGC 300 reported by Soemitro et al. (2023), as both datasets were derived using the same method. Most of the NGC 5128 points fall within the region defined by the MW despite the approximations made to infer their parameters. The distribution does not include objects in the high luminosity CSPNe region, most likely due to the underestimation of the stellar luminosity as a consequence of the optically thick assumption. On the other hand, when considering their effective temperatures, we find – similarly to what is observed in the Magellanic Clouds – that some objects reach high temperatures (see Sec. 3.1).

3.4. Local Group spiral galaxies

Figure 4 shows the HR diagram of the local group spiral galaxies, in particular for M 31 and M 33. Given the limited sample size, our ability to draw meaningful conclusions is restricted. In any case, the points lie within the region defined by the CSPNe of the MW; that is, they do not exhibit anomalous values as seen in the cases of the LMC, SMC, NGC 300, and NGC 5128. Nevertheless, the distribution of points appears to be tightly clustered

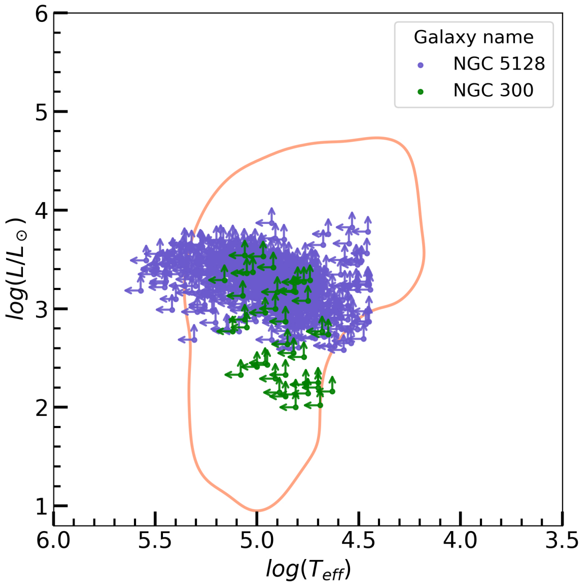

Fig. 3. Hertzsprung–Russell diagram for NGC 5128 and NGC 300. The values were calculated using the equations defined in Sec. 3.2.

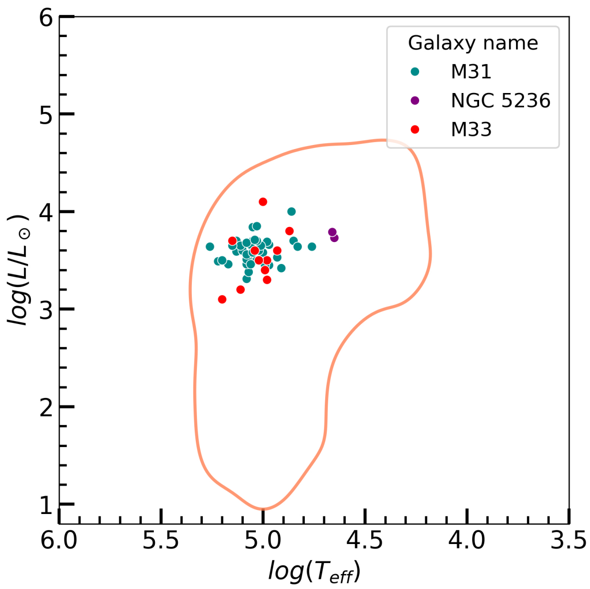

Fig. 4. Hertzsprung–Russell diagram for the spiral galaxies.

in a region characterised by luminosities of log(L/$L_\odot$) ~ 3.2–3.8 and effective temperatures of log(T_{eff}) ~ 4.8–5.2. A possible explanation for this concentration could be a bias introduced by the method used to infer the stellar parameters or by the spatial distribution of the PNe within their host galaxies. However, the data come from four different authors, making a methodological bias unlikely. Furthermore, an inspection of the PNe positions shows that they are not confined to a specific region but rather randomly distributed throughout the galaxies.

3.5. Assessing the accuracy of CSPN parameter estimates

The expressions used to estimate luminosity and temperature (Eqs. 4 and 6) are affected by several assumptions. In this sense, these determinations are only meaningful in a statistical context involving a significant number of objects, as is the case for NGC 300 and NGC 5128.

The expression used to derive the temperature from the excitation class (Eq. 4) is an empirical relation. In Reid & Parker (2010b), the authors analyse (considering the uncertainties involved) this temperature determination method and compare it with the Zanstra temperature (see their Fig. 18). In this context, they showed that for optically thick objects, there is a good correlation between the two temperature determinations, while for optically thin objects, the uncertainty exceeds 50%.

Regarding luminosity, the uncertainty depends on the uncertainty in measuring the 5007Å flux and on the uncertainty in determining the distance to the host galaxy. However, the main source of uncertainty arises from the proportionality constant in Eq. 6. While we can be certain that the uncertainty in this constant is large, assigning it a precise value remains purely speculative (Dopita et al. 1992). For example, if we assume a large uncertainty for the proportionality constant (i.e. 50%), then by propagating the errors we obtain $\sigma(L/L_\odot) \approx 0.7(L/L_\odot)$.

4. Discussion

As can be seen from Figs. 2, 3 and 4, the MW sample of CSPNe is slightly cooler compared to the other galaxies. This difference can be explained by the fact that extragalactic PNe are generally detected through narrowband filters, particularly those centred on [O III]λ5007. Since the ionisation potential for this ion is 35.1 eV, using Eq. 1, we find that only extragalactic CSPNe with temperatures above ≈35,100 K can be detected, corresponding to $\log(T_{eff}) > 4.5$, which aligns with our findings.

As mentioned in Sec. 3.1, except for the points with temperatures below 35100 K and the region corresponding to white dwarfs, the physical parameters of CSPNe in the LMC and SMC are distributed within the same region of the HR diagram as those of the MW. This is not the case for NGC 300 and NGC 5128 (Fig. 3), whose objects are concentrated in a more restricted area. In particular, in NGC 300, objects with log(L/$L_\odot$)<2.5 are likely underestimated, as this region corresponds to white dwarfs (see Fig. 9 of Weidmann et al. 2020). In the case of NGC 5128, the clustering of points may be the result of systematic errors in the luminosity estimates, which are likely introduced by the assumptions made during their determination.

Concerning the effective temperature, according to Eq. 4, when the EC exceeds a value of ten, we are likely dealing with objects hotter than 250×10^3 K. This temperature lies at the upper limit of the evolutionary models presented by Miller Bertolami (2016) for stellar masses greater than 0.8 $M_\odot$. Moreover, one of the hottest known stars, WR102, has an effective temperature of 210 kK (see Table 4 of Tramper et al. 2015). In this context, temperatures derived from EC values above ten should be treated with caution.

5. Conclusions

For the first time, the available data on extragalactic CSPNe have been analysed collectively. In addition to compiling information from the literature, physical parameters were computed for over 1000 objects. Perhaps the most paradigmatic case is that of the Magellanic Clouds, where, for the first time, the physical parameters of 168 known CSPNe – gathered from 11 different papers – are presented together in an HR diagram. This catalogue constitutes a necessary complement to the catalogue of Galactic CSPNe (Weidmann et al. 2020).

In addition to the effective temperature and luminosity, we have included a handful of CSPNe with determined spectral types that have been reported in the literature. In fact, only 4% of the total sample of 1073 objects have a known spectral type. Moreover, in some cases, only specific spectral features are reported, such as a P-Cygni profile or broad Hα emission. The latter are part of the aforementioned 4%.

Although the spectral types of only a few CSPNe have been accurately determined, it is clear that in the LMC, there are 11 objects with a [WC] central star. Of these, five are classified as [WC 5-8], indicating a relatively high proportion of intermediate subtypes compared to the distribution observed in our Galaxy (Weidmann et al. 2020). While [WC] stars are easier to identify due to their strong emission lines (Werner et al. 2024), previous studies (e.g. Zijlstra et al. 2006, that studied the PNe population of the Sagittarius dwarf spheroidal galaxy) suggest that these spectral types are more frequent in metal-poor environments. Metallicities could also explain the presence of CSPNe of an intermediate subtype rarely found in the MW in the LMC (Monk et al. 1988). In this sense, the SMC, which is more metal poor than the LMC (Table 1), should host a higher proportion of these spectral subtypes. However, only two [WC 5–8] detections have been reported in the SMC out of a total of 47 CSPNe, so no firm conclusions can be drawn given the small number of this sample. However, it is important to reiterate that the compiled catalogue is biased towards brighter stars, and therefore, drawing conclusions about relative population fractions based on metallicity remains highly uncertain.

Objects with high surface temperatures were identified in Magellanic Clouds and NGC 5128. If confirmed to be CSPNe, these sources would represent highly unusual cases due to their potentially high masses, and therefore warrant detailed follow-up with large telescopes. Such targeted observations could yield valuable data, offering new insights into stellar evolution.

In summary, the catalogue presented here is expected to serve as a valuable resource for guiding future studies, providing a comprehensive and homogeneous compilation of physical parameters for over a thousand CSPNe. It lays the groundwork for targeted spectroscopic follow-up, refined stellar evolution modelling, and comparative analyses across different galactic environments.

Acknowledgements. We are grateful to the anonymous referee for their valuable feedback, which greatly enhanced this manuscript. WW thanks Luis Gutiérrez-Soto for his support. This work was partially supported by grants PICT 2021-00442 awarded by Foncyt, grant PIP 2022 11220210100520CO by CONICET, and by grant SeCyT UNC Consolidar project 2023 NRO: 33620230100103CB. This research has made use of NASA's Astrophysics Data System Service. This research has made use of the SIMBAD database, operated at CDS, Strasbourg, France.

The catalogue is only available in electronic form at the CDS via anonymous ftp to cdsarc.u-strasbg.fr (130.79.128.5) or via http://cdsweb.u-strasbg.fr/cgi-bin/qcat?J/A+A/.

References

Acker, A., Jasniewicz, G., Koeppen, J., & Stenholm, B. 1989, A&AS, 80, 201
Appleton, P. N., Davies, R. D., & Stephenson, R. J. 1981, MNRAS, 195, 327
Arnaboldi, M., Gerhard, O., Okamura, S., et al. 2007, PASJ, 59, 419
Balick, B., Kwitter, K. B., Corradi, R. L. M., & Henry, R. B. C. 2013, ApJ, 774, 3
Beasley, M. A., Fahrion, K., & Gvozdenko, A. 2024, MNRAS, 527, 5767
Bianchi, L., Vassiliadis, E., & Dopita, M. 1997, ApJ, 480, 290
Choudhury, S., de Grijs, R., Rubele, S., et al. 2020, MNRAS, 497, 3746
Ciardullo, R., Durrell, P. R., Laychak, M. B., et al. 2004, ApJ, 614, 167
Ciardullo, R., Jacoby, G. H., Ford, H. C., & Neill, J. D. 1989, ApJ, 339, 53
Ciardullo, R., Sigurdsson, S., Feldmeier, J. J., & Jacoby, G. H. 2005, ApJ, 629, 499
de Vaucouleurs, G., de Vaucouleurs, A., Corwin, Herold G., J., et al. 1991, Third Reference Catalogue of Bright Galaxies
Delgado-Inglada, G., García-Rojas, J., Stasińska, G., & Rechy-García, J. S. 2020, MNRAS, 498, 5367
Dopita, M. A., Ford, H. C., & Webster, B. L. 1985, ApJ, 297, 593
Dopita, M. A., Jacoby, G. H., & Vassiliadis, E. 1992, ApJ, 389, 27
Dopita, M. A. & Meatheringham, S. J. 1991a, ApJ, 374, L21
Dopita, M. A. & Meatheringham, S. J. 1991b, ApJ, 367, 115
Dopita, M. A. & Meatheringham, S. J. 1991c, ApJ, 377, 480
Dopita, M. A., Vassiliadis, E., Wood, P. R., et al. 1997, ApJ, 474, 188
Fang, X., García-Benito, R., Guerrero, M. A., et al. 2018, ApJ, 853, 50
Ferland, G. J., Korista, K. T., Verner, D. A., et al. 1998, PASP, 110, 761
Flores-Durán, S. N., Peña, M., & Ruiz, M. T. 2017, A&A, 601, A147
Ford, H., Peng, E., & Freeman, K. 2002, in Astronomical Society of the Pacific Conference Series, Vol. 273, The Dynamics, Structure & History of Galaxies: A Workshop in Honour of Professor Ken Freeman, ed. G. S. Da Costa, E. M. Sadler, & H. Jerjen, 41
Freedman, W. L., Madore, B. F., Gibson, B. K., et al. 2001, ApJ, 553, 47
Frew, D. J. & Parker, Q. A. 2010, PASA, 27, 129
Galera-Rosillo, R., Mampaso, A., Corradi, R. L. M., et al. 2022, A&A, 657, A71
Geha, M., van der Marel, R. P., Guhathakurta, P., et al. 2010, ApJ, 711, 361
Gesicki, K., Zijlstra, A. A., & Miller Bertolami, M. M. 2018, Nature Astronomy, 2, 580
Gładkowski, M., Hajduk, M., Smolec, R., Szczerba, R., & Soszyński, I. 2024, A&A, 682, A70
Gonçalves, D. R., Magrini, L., Leisy, P., & Corradi, R. L. M. 2007, MNRAS, 375, 715
Gonçalves, D. R., Magrini, L., Teodorescu, A. M., & Carneiro, C. M. 2014, MNRAS, 444, 1705
González-Santamaría, I., Manteiga, M., Manchado, A., et al. 2021, A&A, 656, A51
Hajduk, M., Gładkowski, M., & Soszyński, I. 2014, A&A, 561, A8
Hamann, W. R. 1996, in Astronomical Society of the Pacific Conference Series, Vol. 96, Hydrogen Deficient Stars, ed. C. S. Jeffery & U. Heber, 127
Hamann, W. R., Peña, M., Gräfener, G., & Ruiz, M. T. 2003, A&A, 409, 969
Harris, J. & Zaritsky, D. 2009, AJ, 138, 1243
Herald, J. E. & Bianchi, L. 2004, ApJ, 611, 294
Hui, X., Ford, H. C., Ciardullo, R., & Jacoby, G. H. 1993, ApJS, 88, 423
Hyung, S., Aller, L. H., Han, S.-R., et al. 2000, Journal of Korean Astronomical Society, 33, 97
Idiart, T. P., Maciel, W. J., & Costa, R. D. D. 2007, A&A, 472, 101
Iłkiewicz, K., Mikołajewska, J., Miszalski, B., Kozłowski, S., & Udalski, A. 2018, MNRAS, 476, 2605
Jacoby, G. H. 1989, ApJ, 339, 39
Jacoby, G. H. & Ciardullo, R. 1999, ApJ, 515, 169
Jones, O. C., Álvarez-Márquez, J., Sloan, G. C., et al. 2023, MNRAS, 523, 2519
Kniazev, A. Y., Grebel, E. K., Pustilnik, S. A., & Pramskij, A. G. 2007, A&A, 468, 121
Kwitter, K. B. & Henry, R. B. C. 2022, PASP, 134, 022001
Kwitter, K. B., Lehman, E. M. M., Balick, B., & Henry, R. B. C. 2012, ApJ, 753, 12
Kwok, S. 2007, The Origin and Evolution of Planetary Nebulae
Larsen, S. S. & Richtler, T. 2006, A&A, 459, 103
Licquia, T. C. & Newman, J. A. 2015, ApJ, 806, 96
Magrini, L. 2006, in IAU Symposium, Vol. 234, Planetary Nebulae in our Galaxy and Beyond, ed. M. J. Barlow & R. H. Méndez, 9–16
Magrini, L., Leisy, P., Corradi, R. L. M., et al. 2005, A&A, 443, 115
Magrini, L., Perinotto, M., Mampaso, A., & Corradi, R. L. M. 2004, A&A, 426, 779
Margon, B., Manea, C., Williams, R., et al. 2020a, ApJ, 888, 54
Margon, B., Massey, P., Neugent, K. F., & Morrell, N. 2020b, ApJ, 898, 85
Margon, B., Morrell, N., Massey, P., Neugent, K. F., & Williams, R. 2023, ApJ, 942, 85
Mateo, M. L. 1998, ARA&A, 36, 435
Mazzi, A., Girardi, L., Zaggia, S., et al. 2021, MNRAS, 508, 245
McConnachie, A. W. 2012, AJ, 144, 4
Melekh, B. Y., Holovatyy, V. V., Havrylova, N. V., et al. 2012, Odessa Astronomical Publications, 25, 178
Mendez, R. H., Kudritzki, R. P., Herrero, A., Husfeld, D., & Groth, H. G. 1988, A&A, 190, 113
Merrett, H. R., Merrifield, M. R., Douglas, N. G., et al. 2006, MNRAS, 369, 120
Miller Bertolami, M. M. 2016, A&A, 588, A25
Miszalski, B., Napiwotzki, R., Cioni, M. R. L., et al. 2011, A&A, 531, A157
Monk, D. J., Barlow, M. J., & Clegg, R. E. S. 1988, MNRAS, 234, 583
Murset, U. & Nussbaumer, H. 1994, A&A, 282, 586
Ostlie, D. A. & Carroll, B. W. 1996, An Introduction to Modern Stellar Astrophysics
Otsuka, M., Kemper, F., Leal-Ferreira, M. L., et al. 2016, MNRAS, 462, 12

Peña, M. & Hamann, W. R. 2004, in Revista Mexicana de Astronomia y Astrofisica Conference Series, Vol. 20, Revista Mexicana de Astronomia y Astrofisica Conference Series, ed. G. Tovmassian & E. Sion, 41–43
Peña, M., Stasińska, G., & Richer, M. G. 2007, A&A, 476, 745
Pena, M., Ruiz, M. T., & Torres-Peimbert, S. 1997, A&A, 324, 674
Reid, W. A. & Parker, Q. A. 2010a, MNRAS, 405, 1349
Reid, W. A. & Parker, Q. A. 2010b, PASA, 27, 187
Richer, H. B., Pritchet, C. J., & Crabtree, D. R. 1985, ApJ, 298, 240
Richer, M. G. & McCall, M. L. 2008, ApJ, 684, 1190
Rolleston, W. R. J., Trundle, C., & Dufton, P. L. 2002, A&A, 396, 53
Saviane, I., Exter, K., Tsamis, Y., Gallart, C., & Péquignot, D. 2009, A&A, 494, 515
Schönberner, D., Jacob, R., Sandin, C., & Steffen, M. 2010, A&A, 523, A86
Shenar, T. 2024, arXiv e-prints, arXiv:2410.04436
Soemitro, A. A., Roth, M. M., Weilbacher, P. M., et al. 2023, A&A, 671, A142
Spiniello, C., Napolitano, N. R., Arnaboldi, M., et al. 2018, MNRAS, 477, 1880
Stanghellini, L. & Haywood, M. 2010, ApJ, 714, 1096
Stanghellini, L., Lee, T.-H., Shaw, R. A., Balick, B., & Villaver, E. 2009, ApJ, 702, 733
Stanghellini, L., Magrini, L., Villaver, E., & Galli, D. 2010, A&A, 521, A3
Stanghellini, L., Shaw, R. A., Balick, B., et al. 2003, ApJ, 596, 997
Stanghellini, L., Shaw, R. A., & Gilmore, D. 2005, ApJ, 622, 294
Taibi, S., Roth, M. M., Battaglia, G., & Kamann, S. 2024, Research Notes of the American Astronomical Society, 8, 45
Tosi, S., Dell'Agli, F., Kamath, D., et al. 2024, A&A, 688, A36
Tramper, F., Straal, S. M., Sanyal, D., et al. 2015, A&A, 581, A110
Valenzuela, L. M., Miller Bertolami, M. M., Remus, R.-S., & Méndez, R. H. 2025, arXiv e-prints, arXiv:2501.17926
Villaver, E., Stanghellini, L., & Shaw, R. A. 2003, ApJ, 597, 298
Villaver, E., Stanghellini, L., & Shaw, R. A. 2004, ApJ, 614, 716
Villaver, E., Stanghellini, L., & Shaw, R. A. 2007, ApJ, 656, 831
Walsh, J. R., Rejkuba, M., & Walton, N. A. 2015, A&A, 574, A109
Wang, Q. 1991, MNRAS, 252, 47P
Weidmann, W. A. & Gamen, R. 2011, A&A, 526, A6
Weidmann, W. A., Mari, M. B., Schmidt, E. O., et al. 2020, A&A, 640, A10
Werner, K., Todt, H., Bond, H. E., & Zeimann, G. R. 2024, A&A, 686, A29
Zijlstra, A. A., Gesicki, K., Walsh, J. R., et al. 2006, MNRAS, 369, 875
Zijlstra, A. A., van Hoof, P. A. M., Chapman, J. M., & Loup, C. 1994, A&A, 290, 228

Appendix A: Catalogue of extragalactic CSPNe

Table A.1. Catalogue of extragalactic CSPNe. Description of the columns is in Section 2, t.w. means this work.

Name	galaxy	RA_{J2000}	DEC_{J2000}	log T_{eff}	Ref.	log($L/L_{\odot}$)	Ref.	SpT	Ref.	RB	comm.
DDHW 1	Fornax	02 39 49.30	−34 32 47.00	4.74	KG07	3.85	KG07	wels?	KG07		
x-x	IC 1613							K giant + ?	TR24	TR24	
LMC-SMP 104A	LMC	04 25 32.15	−66 47 18.50	4.89	VS07	4.69	VS07				
LMC-SMP 1	LMC	04 38 34.79	−70 36 43.28					[WC 4]	MM23		
LMC-SMP 2	LMC	04 40 56.69	−67 48 02.17	4.58	HB04	3.42	HB04				
LMC-SMP 3	LMC	04 42 24.00	−66 13 01.66	4.67	DM91c	3.00	DM91c				
LMC-SMP 4	LMC	04 43 21.89	−71 30 08.89	5.02	TD24	3.81	TD24				
LMC-SMP 6	LMC	04 47 38.98	−72 28 20.57	5.15	DM91c	3.79	DM91c				
LMC-SMP 5	LMC	04 48 08.62	−67 26 06.50	4.74	VS07	4.07	VS07				
LMC-SMP 7	LMC	04 48 29.61	−69 08 12.97	5.35	DM91c	3.41	DM91c				
[M94b] 7	LMC	04 49 19.86	−64 22 36.80	4.47	VS07	2.23	VS07				[1]
LMC-SMP 8	LMC	04 50 13.15	−69 33 56.77	4.72	DV97	3.59	DV97				
LMC-SMP 9	LMC	04 50 24.67	−68 13 16.44	5.06	VS03	< 3.25	VS03				
LMC-SMP 10	LMC	04 51 08.92	−68 49 05.42	4.87	VS03	3.29	VS03				
LMC-SMP 11	LMC	04 51 37.83	−67 05 16.88					SySt?	DF85		[2]
LMC-SMP 13	LMC	04 59 59.99	−70 27 40.80	5.11	VS03	3.51	VS03				
LMC-SMP 14	LMC	05 00 20.73	−70 58 51.40	5.42	DM91c	2.85	DM91c				
LMC-SMP 15	LMC	05 00 52.66	−70 13 40.98	5.13	DM91	3.83	DM91				
MGPN LMC 12	LMC	05 01 40.22	−66 46 46.00					hot CSPN	MN11		
LMC-SMP 16	LMC	05 02 01.98	−69 48 53.60	5.15	VS03	< 3.54	VS03				
MGPN LMC 13	LMC	05 03 03.23	−65 23 02.86					hot CSPN	MN11		
LMC-SMP 19	LMC	05 03 41.23	−70 13 53.45	5.16	VS03	3.45	VS03				
LMC-SMP 18	LMC	05 03 42.63	−70 06 47.49	4.70	TD24	3.30	TD24	P-Cygni	SS05		
MGPN LMC 14	LMC	05 04 27.67	−68 58 12.30	4.77	VS07	2.92	VS07				
[RP2006] 1773	LMC	05 04 35.10	−70 06 19.10							GH24	
LMC-SMP 20	LMC	05 04 40.47	−69 21 39.10	5.18	DV97	3.52	DV97				
LMC-SMP 21	LMC	05 04 51.99	−68 39 09.70	5.28	MH12	3.16	MH12				
MGPN LMC 16	LMC	05 06 05.22	−64 48 48.90	4.74	VS07	2.12	VS07				
LMC-SMP 23	LMC	05 06 09.44	−67 45 27.80	4.78	HB04	3.77	HB04				
LMC-SMP 24	LMC	05 06 18.27	−68 59 30.90	5.30	DM91c	2.72	DM91c				
LMC-SMP 25	LMC	05 06 23.90	−69 03 19.17	4.78	TD24	3.69	TD24	P-Cygni	SS05		
LMC-SMP 107	LMC	05 06 43.81	−69 15 38.40	4.75	VS07	3.23	VS07				
TIC 40274393	LMC	05 07 38.92	−68 26 06.14					[WCL] ?	MM20		[3]
LMC-SMP 27	LMC	05 07 54.86	−66 57 45.52	4.45	VS03	2.95	VS03	P-Cygni	SS05		
LMC-SMP 28	LMC	05 07 57.62	−68 51 47.43	4.23	VS03						
LMC-SMP 29	LMC	05 08 03.35	−68 40 16.56	5.30	DM91c	3.52	DM91c				
LMC-SMP 30	LMC	05 09 10.54	−66 53 38.40	5.17	VS03	2.65	VS03				
LMC-SMP 31	LMC	05 09 20.20	−67 47 25.09	4.46	VS03	3.62	VS03				
LMC-SMP 32	LMC	05 09 37.23	−70 49 08.43	5.27	DM91c	3.48	DM91c				
LMC-SMP 33	LMC	05 10 09.43	−68 29 54.55	5.05	VS03	< 4.06	VS03				
LMC-SMP 34	LMC	05 10 17.05	−68 48 22.42	4.66	TD24	3.69	TD24	P-Cygni	SS05		

Continued on next page

[1] PN Candidate.
[2] SySt?
[3] Hot, H-poor, post-AGB star. It is possible that it is caught in transition from a late [WC] star to a hot white dwarf.

Table A.1 – continued.

Name	galaxy	RA_{J2000}	DEC_{J2000}	log T_{eff}	Ref.	log($L/L_\odot$)	Ref.	SpT	Ref.	RB	comm.
LMC-SMP 35	LMC	05 10 49.93	−65 29 30.87	4.78	HB04	3.01	HB04				
LMC-SMP 37	LMC	05 11 02.91	−67 47 59.38	5.19	DM91	3.53	DM91				4
LMC-SMP 38	LMC	05 11 23.69	−70 01 57.36	4.85	PR97	3.52	DM91c	[WC 5]	MM23		
LMC-SMP 109	LMC	05 11 48.05	−69 23 42.20	4.79	VS07	4.33	VS07				
LMC-SMP 40	LMC	05 12 15.69	−66 22 56.60	5.25	DV97	3.12	DV97				
LMC-SMP 41	LMC	05 13 27.23	−70 33 35.00	5.24	DM91c	2.77	DM91c				
MGPN LMC 29	LMC	05 13 42.48	−68 15 17.90	5.24	VS07	2.82	VS07				
[RP2006] 1488	LMC	05 13 57.12	−68 25 09.00							GH24	
LMC-SMP 42	LMC	05 15 46.75	−68 42 23.52	4.82	VS03	3.82	VS03				
LMC-SMP 43	LMC	05 17 02.40	−69 07 16.10	4.82	VS07	2.95	VS07				
LMC-SMP 44	LMC	05 18 29.94	−67 16 55.80	5.24	DM91c	2.48	DM91c				
[RP2006] 1429	LMC	05 19 18.62	−68 49 12.10							GH24	
LMC-SMP 45	LMC	05 19 20.75	−66 58 08.40	5.12	VS07	2.93	VS07				
LMC-SMP 46	LMC	05 19 29.63	−68 51 09.02	5.08	VS03	< 3.65	VS03				
LMC-SMP 47	LMC	05 19 54.63	−69 31 04.99	5.15	DV97	3.68	DV97				
LMC-SMP 49	LMC	05 20 09.46	−70 25 38.50	5.13	VS07	2.99	VS07				
LMC-SMP 48	LMC	05 20 09.51	−69 53 39.14	4.77	DM91c	3.57	DM91c	P-Cygni	SS05		
LMC-SMP 50	LMC	05 20 51.72	−67 05 43.34	4.91	VS03	4.11	VS03				
LMC-SMP 51	LMC	05 20 52.43	−70 09 35.49					[WC 4–5]	MM23		
LMC-SMP 115	LMC	05 21 18.11	−69 43 01.90	4.94	VS07	3.38	VS07				
LMC-SMP 52	LMC	05 21 23.96	−68 35 33.79	5.00	VS03	4.00	VS03				
LMC-SMP 53	LMC	05 21 32.85	−67 00 04.75	4.64	VS03	< 3.63	VS03				
LMC-SMP 54	LMC	05 21 42.82	−68 39 24.71	5.36	DM91c	2.90	DM91c				
MGPN LMC 40	LMC	05 22 35.36	−68 24 26.50	4.81	VS07	3.01	VS07				
[RP2006] 979	LMC	05 22 38.97	−67 55 09.20							GH24	
LMC-SMP 55	LMC	05 22 40.98	−71 19 06.63	4.57	DM91c	3.69	DM91c				
LMC-SMP 56	LMC	05 23 31.26	−69 04 08.85	4.66	VS03	3.89	VS03				
LMC-SMP 57	LMC	05 23 48.69	−69 12 20.90	4.79	VS07	3.46	VS07				
LMC-SMP 60	LMC	05 24 15.64	−70 53 55.94	5.41	DM91c	3.31	DM91c				
LMC-SMP 58	LMC	05 24 20.74	−70 05 01.60	5.20	JA23	3.73	ZV94	[WC 5]	MM23		
LMC-SMP 59	LMC	05 24 27.26	−70 22 23.90	4.99	VS03	3.86	VS03			GH24	
LMC-SMP 61	LMC	05 24 36.37	−73 40 40.00	4.76	VS07	4.02	VS07	[WC 5-6]	PR97		
LMC-SMP 62	LMC	05 24 55.10	−71 32 56.32	4.65	HB04	3.73	HB04				
LMC-SMP 117	LMC	05 24 56.82	−69 15 31.20	4.90	VS07	2.62	VS07				
LMC-SMP 63	LMC	05 25 26.12	−68 55 55.40	4.64	VS07	3.71	VS07				
MGPN LMC 45	LMC	05 26 06.45	−63 24 04.40	4.73	VS07	4.91	VS07				5
LMC-SMP 64	LMC	05 27 35.65	−69 08 56.38	4.50	DM91b	3.82	DM91b			GH24	
LMC-SMP 65	LMC	05 27 43.81	−71 25 56.50	4.43	VS03	3.12	VS03				
MGPN LMC 51	LMC	05 28 34.47	−70 33 01.90	4.67	VS07	3.18	VS07				
LMC-SMP 66	LMC	05 28 41.20	−67 33 39.00	5.03	TD24	3.65	TD24				
[RP2006] 695	LMC	05 28 44.20	−69 54 22.50							GH24	
LMC-SMP 68	LMC	05 29 02.83	−70 19 23.80	5.21	VS07	3.37	VS07				
LMC-SMP 67	LMC	05 29 16.01	−67 32 48.00	4.69	VS07	3.40	VS07	P-Cygni ?	BV97		
LMC-SMP 121	LMC	05 30 26.20	−71 13 49.50	5.01	VS07	1.64	VS07				
LMC-SMP 71	LMC	05 30 33.17	−70 44 37.90	5.21	TD24	3.73	TD24				
LMC-SMP 72	LMC	05 30 45.84	−70 50 16.53	5.26	DM91c	2.96	DM91c				
MGPN LMC 55	LMC	05 31 09.07	−71 36 40.40							GH24	

Continued on next page

[4] post-AGB?
[5] The coordinates of CDS and paper are different in DEC.

Table A.1 – continued.

Name	galaxy	RA_{J2000}	DEC_{J2000}	log T_{eff}	Ref.	$\log(L/L_{\odot})$	Ref.	SpT	Ref.	RB	comm.
TIC 425061481	LMC	05 31 21.76	−70 17 39.93					[WC 11]	MM20		6
LMC-SMP 73	LMC	05 31 21.89	−70 40 45.47	5.13	DM91c	3.85	DM91c				
[M94b] 30	LMC	05 31 35.18	−69 23 46.60							GH24	
[M94b] 33	LMC	05 32 09.75	−70 24 43.70	5.26	VS07	2.39	VS07				
LMC-SMP 74	LMC	05 33 29.51	−71 52 27.90	5.02	VS07	3.82	VS07				
LMC-SMP 76	LMC	05 33 56.10	−67 53 08.83	4.76	DV97	3.73	DV97	P-Cygni ?	BV97		
LMC-SMP 77	LMC	05 34 06.26	−69 26 18.25	4.66	DM91	3.42	DM91				
LMC-SMP 79	LMC	05 34 08.61	−74 20 06.73	4.53	VS03	< 3.79	VS03	P-Cygni	SS05		
LMC-SMP 78	LMC	05 34 21.18	−68 58 25.30	4.88	VS03	< 4.61	VS03				
LMC-SMP 80	LMC	05 34 38.84	−70 19 56.70	4.76	TD24	3.50	TD24	P-Cygni	SS05		
LMC-SMP 81	LMC	05 35 20.86	−73 55 30.25	4.90	TD24	3.67	TD24	P-Cygni	SS05		
LMC-SMP 82	LMC	05 35 57.47	−69 58 16.60	4.82	VS07	4.21	VS07				
LMC-SMP 83	LMC	05 36 20.82	−67 18 07.00	5.06	VS07	3.99	VS07	[WN 4.5]	HP03		7
LMC-SMP 84	LMC	05 36 53.17	−71 53 39.80	4.71	VS07	3.96	VS07				
LMC-SMP 85	LMC	05 40 30.81	−66 17 37.26	4.60	HB04	3.41	HB04	[WC 8]	MM23		
LMC-SMP 87	LMC	05 41 08.04	−72 42 08.29	5.23	DV97	3.69	DV97				
LMC-SMP 88	LMC	05 42 33.19	−70 29 24.08	4.80	VS07	4.66	VS07		IM18	IM18	8
LMC-SMP 89	LMC	05 42 36.65	−70 09 32.13	5.00	DM91	3.93	DM91				
MGPN LMC 77	LMC	05 43 47.57	−68 38 35.10					hot CSPN	MN11		
LMC-SMP 92	LMC	05 47 04.80	−69 27 32.10	5.15	DM91c	3.96	DM91c				
LMC-SMP 93	LMC	05 49 38.85	−69 10 00.25	5.57	VS03	< 3.04	VS03				
LMC-SMP 94	LMC	05 54 09.52	−73 02 34.16	4.77	VS03	5.21	VS03	SySt?	DF85		9
[M94b] 41	LMC	05 55 13.68	−65 28 23.22	5.00	H96	3.80	H96	[WC 7]	PR97		
[M94b] 42	LMC	05 55 14.63	−66 50 25.08					hot CSPN	MN11		10
TIC 31531046	LMC	05 58 25.98	−69 44 25.82					[WC 11]	MM23		11
LMC-SMP 95	LMC	06 01 45.34	−67 56 06.40	5.16	VS03	< 3.08	VS03				
LMC-SMP 96	LMC	06 06 05.70	−71 04 17.00	5.40	DM91	2.98	DM91				
TIC 41258976	LMC	06 08 19.94	−71 57 37.45					[WC 11]	MM20		12
LMC-SMP 97	LMC	06 10 25.42	−67 56 20.88	5.24	DM91	3.78	DM91				
[M94b] 47	LMC	06 13 03.35	−65 55 09.40	5.39	VS07	2.26	VS07				
LMC-SMP 99	LMC	06 18 58.02	−71 35 50.52	5.09	DM91c	3.76	DM91c				
[M94b] 49	LMC	06 21 04.71	−66 08 00.73	5.00	PR97			WC-Of ?	PR97		
LMC-SMP 100	LMC	06 22 55.46	−72 07 41.03	5.10	VS03	3.47	VS03				
LMC-SMP 101	LMC	06 23 40.24	−69 10 38.90	4.99	VS07	4.07	VS07				
LMC-SMP 102	LMC	06 29 32.91	−68 03 32.76	5.15	TD24	3.56	TD24				
[MMD2006] 2538	M 31	00 36 28.80	+39 35 26.40	5.11	GM22	3.65	GM22				
[MMD2006] 1985	M 31	00 37 51.30	+40 45 48.10	5.05	KL12	3.84	KL12				
[MMD2006] 2694	M 31	00 38 46.20	+41 28 19.60	5.03	KL12	3.85	KL12				
[MMD2006] 2860	M 31	00 38 55.00	+41 06 55.30	5.08	GM22	3.51	GM22				
[MMD2006] 174	M 31	00 39 01.00	+41 51 11.10	4.85	BK13	3.70	BK13				
[MMD2006] 1583	M 31	00 39 22.60	+41 06 57.30	5.15	KL12	3.65	KL12				

Continued on next page

6 There is no PN reported in the literature, but multiple forbidden lines in our spectrum indicates that a low-density region is certainly present (MM23).
7 Thermal pulse in progress - variability in L and T_{eff} (PM04).
8 D'-type SySt?
9 SySt?
10 Bipolar PNe. The VMC image of Mo42 reveals a central star that is brightest in Y band. Peimbert type I.
11 No nebula has been reported (MM23).
12 Although no obvious surrounding nebulosity is present in J0608, [OII], [NII], and [$S\,II$] emission suggest the presence of an inconspicuous, low-excitation nebula (MMb20).

Table A.1 – continued.

Name	galaxy	RA_{J2000}	DEC_{J2000}	log T_{eff}	Ref.	log($L/L_{\odot}$)	Ref.	SpT	Ref.	RB	comm.
[MMD2006] 1596	M 31	00 39 22.60	+41 06 57.30	5.22	GM22	3.49	GM22				
[MMD2006] 1596	M 31	00 40 00.80	+41 04 09.30	5.06	KL12	3.46	KL12				
[MMD2006] 795	M 31	00 40 26.20	+41 20 27.80	5.03	KL12	3.70	KL12				
[MMD2006] 1074	M 31	00 40 38.10	+41 16 48.00	5.03	GM22	3.50	GM22				
[MMD2006] 2068	M 31	00 40 49.60	+40 39 46.50	5.05	GM22	3.62	GM22				
[MMD2006] 2690	M 31	00 40 58.70	+41 29 32.40	5.01	KL12	3.65	KL12				
[MMD2006] 2240	M 31	00 41 01.80	+40 24 20.40	5.08	KL12	3.68	KL12				
[MMD2006] 337	M 31	00 41 41.00	+41 38 14.80	5.04	KL12	3.71	KL12				
[MMD2006] 553	M 31	00 41 54.50	+41 36 16.70	5.02	KL12	3.60	KL12				
[MMD2006] 2624	M 31	00 42 15.10	+41 39 10.10	5.26	KL12	3.64	KL12				
[MMD2006] 2750	M 31	00 42 40.30	+41 19 07.40	4.99	FG18	3.45	FG18				
[MMD2006] 71	M 31	00 42 59.00	+42 02 14.20	5.05	KL12	3.58	KL12				
[MMD2006] 586	M 31	00 43 07.90	+41 28 45.50	5.05	FG18	3.70	FG18				
[MMD2006] 2471	M 31	00 43 11.20	+42 20 45.70	5.20	GM22	3.50	GM22				
[MMD2006] 1675	M 31	00 43 15.20	+41 04 21.50	5.10	GM22	3.60	GM22				
[MMD2006] 1687	M 31	00 43 21.30	+41 05 28.90	5.06	GM22	3.66	GM22				
[MMD2006] 77	M 31	00 43 32.30	+41 58 42.50	4.93	FG18	3.53	FG18				
[MMD2006] 2472	M 31	00 44 02.30	+42 17 16.60	5.00	KL12	3.58	KL12				
[FGG2015] PN10	M 31	00 44 03.10	+42 27 46.60	4.98	FG18	3.69	FG18				
[MMD2006] 2496	M 31	00 44 26.00	+40 15 45.60	4.86	BK13	4.00	BK13				
[MMD2006] 2445	M 31	00 45 52.80	+42 36 52.90	4.97	FG18	3.66	FG18				
[MMD2006] 2512	M 31	00 45 58.50	+39 13 25.40	5.07	FG18	3.38	FG18				
[MMD2006] 2449	M 31	00 46 13.80	+42 40 28.50	5.07	FG18	3.50	FG18				
[MMD2006] 746	M 31	00 46 18.30	+41 31 09.90	5.08	KL12	3.56	KL12				
[MMD2006] 2427	M 31	00 46 26.50	+43 00 43.00	5.13	FG18	3.70	FG18				
[MMD2006] 50	M 31	00 46 42.90	+42 08 35.30	5.13	GM22	3.59	GM22				
[MMD2006] 2451	M 31	00 46 59.30	+42 37 58.20	5.08	FG18	3.46	FG18				
[MMD2006] 2430	M 31	00 47 25.90	+42 58 59.70	5.08	FG18	3.31	FG18				
[MMD2006] 2432	M 31	00 47 30.30	+43 03 40.90	5.14	FG18	3.66	FG18				
[MMD2006] 2507	M 31	00 48 27.20	+39 55 34.30	4.83	FG18	3.64	FG18				
[MMD2006] 2466	M 31	00 49 08.00	+42 28 44.30	4.76	FG18	3.64	FG18				
[FGG2015] PN7	M 31	00 49 29.00	+37 50 45.40	4.97	FG18	3.45	FG18				
[FGG2015] PN13	M 31	00 49 55.20	+38 32 49.00	4.91	FG18	3.42	FG18				
[FGG2015] PN17	M 31	00 53 38.60	+41 09 32.10	5.17	FG18	3.46	FG18				
PN 1	M 32	00 42 35.89	+40 53 00.51	4.93	HA00						[13]
PN 5	M 32	00 42 39.60	+40 52 40.40	4.90	HA00						
PN 6	M 32	00 42 40.40	+40 52 44.00	5.02	HA00						
[FGG2015] PN16	M 32	00 42 42.20	+40 51 39.80	5.24	FG18	3.33	FG18				
PN 24	M 32	00 42 42.56	+40 51 56.52	5.26	HA00						
PN 25	M 32	00 42 42.66	+40 51 56.41	5.22	HA00						[14]
PN 7	M 32	00 42 48.20	+40 54 13.60	4.90	HA00						[15]
PN 2	M 32	00 42 53.00	+40 49 00.00	4.90	HA00						[16]
PN 11	M 32	00 42 56.99	+40 51 01.30	5.00	HA00						
PN 8	M 32	00 43 02.00	+40 49 30.50	4.95	HA00						

Continued on next page

[13] Two model predictions (because there is not a single satisfactory model), we choose the lowest value.
[14] Two model predictions (because there is not a single satisfactory model), we choose the lowest value.
[15] Two model predictions (because there is not a single satisfactory model), we choose the lowest value.
[16] Two model predictions (because there is not a single satisfactory model), we choose the lowest value.

Table A.1 – continued.

Name	galaxy	RA_{J2000}	DEC_{J2000}	log T_{eff}	Ref.	log($L/L_{\odot}$)	Ref.	SpT	Ref.	RB	comm.
PN 8	M 33	01 32 49.20	+30 25 51.00	4.87	MP04	3.80	MP04				
PN 18	M 33	01 33 09.10	+30 31 06.00	5.00	MP04	4.10	MP04				
PN 28	M 33	01 33 19.60	+30 29 39.00	5.15	MP04	3.70	MP04				
PN 60	M 33	01 33 46.10	+30 26 56.00	5.20	MP04	3.10	MP04				
PN 65	M 33	01 33 50.80	+30 32 04.00	5.11	MP04	3.20	MP04				
PN 75	M 33	01 34 01.40	+30 50 22.00	4.98	MP04	3.50	MP04				
PN 91	M 33	01 34 13.80	+30 22 36.00	5.04	MP04	3.60	MP04				
PN 93	M 33	01 34 15.50	+30 24 55.00	4.98	MP04	3.30	MP04				
PN 96	M 33	01 34 16.20	+30 32 17.00	5.02	MP04	3.50	MP04				
PN 101	M 33	01 34 23.30	+30 27 56.00	4.99	MP04	3.40	MP04				
PN 125	M 33	01 34 47.10	+30 41 06.00	4.93	MP04	3.60	MP04				
PN9m	M 81	09 54 46.52	+69 05 39.00	4.50	t.w.	3.61	t.w.				
PN45m	M 81	09 55 21.81	+69 07 50.60	4.46	t.w.	3.53	t.w.				
PN3m	M 81	09 54 26.54	+69 10 30.50	4.49	t.w.	3.31	t.w.				
PN70m	M 81	09 55 30.62	+69 07 56.30	4.50	t.w.	3.61	t.w.				
PN121m	M 81	09 55 51.46	+69 05 14.90	4.51	t.w.	3.65	t.w.				
PN17m	M 81	09 55 10.09	+69 02 37.10	4.47	t.w.	3.38	t.w.				
PN63m	M 81	09 55 28.25	+69 01 26.50	4.49	t.w.	3.37	t.w.				
PN41m	M 81	09 55 02.58	+69 06 26.30	5.15	t.w.	3.57	t.w.				
PN158m	M 81	09 56 32.84	+69 03 58.80	4.86	t.w.	3.39	t.w.				
PN93m	M 81	09 55 39.07	+69 05 42.10	4.46	t.w.	3.69	t.w.				
PN38m	M 81	09 55 19.47	+68 54 45.70	4.74	t.w.	3.32	t.w.				
PN 3	NGC 147	00 32 58.79	+48 27 40.50	5.04	GM07	2.50	GM07				
PN 1	NGC 147	00 32 59.97	+48 32 26.00	4.96	GM07	2.10	GM07				
PN 2	NGC 147	00 33 03.78	+48 31 25.20	4.88	GM07	2.50	GM07				
PN 7	NGC 147	00 33 11.76	+48 32 17.80	4.85	GM07	3.28	GM07				
PN 4	NGC 147	00 33 12.66	+48 28 18.10	4.85	GM07	3.43	GM07				
PN 6	NGC 147	00 33 13.63	+48 30 49.40	4.92	GM07	1.80	GM07				
PN3	NGC 185	00 39 00.23	+48 19 47.30	5.44	t.w.	2.93	t.w.				
F2-3	NGC 205	00 40 02.65	+41 42 13.57	5.23	GM14	2.96	GM14				
F2-7	NGC 205	00 40 14.94	+41 42 02.11	5.29	GM14	2.78	GM14				
F1-8	NGC 205	00 40 08.77	+41 40 43.75	5.05	GM14	4.00	GM14				
F1-9	NGC 205	00 40 13.47	+41 38 42.07	4.96	GM14	4.16	GM14				
Q-1	NGC 300	00 54 22.61	−37 37 52.67	> 4.85	SR23	2.64	SR23				
P-2	NGC 300	00 54 25.37	−37 36 29.93	> 4.92	SR23	3.42	SR23				
H11-2	NGC 300	00 54 37.65	−37 39 03.73	4.65	SR23	2.74	SR23				
I-2	NGC 300	00 54 37.93	−37 40 14.29	> 5.07	SR23	3.13	SR23				
E-11	NGC 300	00 54 38.17	−37 39 41.42	> 5.12	SR23	2.77	SR23				
A-31	NGC 300	00 54 38.95	−37 39 43.26	> 5.05	SR23	2.81	SR23				
A-23	NGC 300	00 54 40.02	−37 40 02.33	> 5.06	SR23	3.54	SR23				
E-2	NGC 300	00 54 41.95	−37 40 43.32	> 4.74	SR23	3.29	SR23				
C-7	NGC 300	00 54 42.24	−37 40 04.82	> 4.90	SR23	3.17	SR23				
H10-2	NGC 300	00 54 43.57	−37 39 35.80	> 4.96	SR23	2.96	SR23				
A-11	NGC 300	00 54 43.66	−37 40 10.98	> 4.80	SR23	3.27	SR23				
E-4	NGC 300	00 54 45.79	−37 41 30.80	> 4.81	SR23	2.00	SR23				
H9-6	NGC 300	00 54 45.85	−37 39 58.04	4.70	SR23	2.20	SR23				
H9-2	NGC 300	00 54 48.11	−37 39 41.62	> 4.86	SR23	2.11	SR23				
H9-1	NGC 300	00 54 48.44	−37 39 48.40	> 4.97	SR23	3.53	SR23				
C-2	NGC 300	00 54 48.98	−37 42 09.55	> 4.76	SR23	2.23	SR23				

Continued on next page

Table A.1 – continued.

Name	galaxy	RA$_{J2000}$	DEC$_{J2000}$	log T$_{eff}$	Ref.	log(L/L$_{\odot}$)	Ref.	SpT	Ref.	RB	comm.
H9-11	NGC 300	00 54 49.31	−37 40 19.15	4.63	SR23	2.16	SR23				
C-6	NGC 300	00 54 52.16	−37 42 43.27	> 4.77	SR23	2.51	SR23				
L14-2	NGC 300	00 54 52.16	−37 41 32.42	> 4.81	SR23	2.13	SR23				
L2-3	NGC 300	00 54 52.90	−37 44 00.13	> 4.91	SR23	3.00	SR23				
H1-8	NGC 300	00 54 53.10	−37 39 34.10	> 4.81	SR23	3.17	SR23				
L9-8	NGC 300	00 54 53.28	−37 40 54.37	> 4.82	SR23	3.18	SR23				
I-5	NGC 300	00 54 53.45	−37 41 56.10	> 4.95	SR23	2.43	SR23				
H2-6	NGC 300	00 54 54.03	−37 39 28.14	> 4.75	SR23	3.08	SR23				
H16-1	NGC 300	00 54 54.22	−37 41 50.64	> 4.89	SR23	2.15	SR23				
B-1	NGC 300	00 54 54.36	−37 42 32.71	> 4.96	SR23	2.45	SR23				
H14-19	NGC 300	00 54 54.95	−37 41 32.88	> 4.68	SR23	2.77	SR23				
H14-18	NGC 300	00 54 55.34	−37 41 28.34	4.82	SR23	2.55	SR23				
H7-3	NGC 300	00 54 56.54	−37 40 29.00	> 5.02	SR23	3.37	SR23				
H7-2	NGC 300	00 54 58.41	−37 40 44.29	> 5.05	SR23	3.36	SR23				
H7-7	NGC 300	00 54 58.44	−37 41 09.84	> 5.06	SR23	2.89	SR23				
H6-9	NGC 300	00 54 59.83	−37 41 00.24	4.70	SR23	2.25	SR23				
H1-3	NGC 300	00 55 00.90	−37 39 39.74	> 5.08	SR23	2.33	SR23				
H6-5	NGC 300	00 55 02.00	−37 40 28.21	> 4.86	SR23	2.87	SR23				
L6-7	NGC 300	00 55 02.42	−37 39 54.64	> 5.16	SR23	3.29	SR23				
H12-2	NGC 300	00 55 03.18	−37 42 08.97	4.75	SR23	2.14	SR23				
H6-1	NGC 300	00 55 04.00	−37 40 41.44	4.69	SR23	2.02	SR23				
H12-14	NGC 300	00 55 04.01	−37 41 51.29	> 5.00	SR23	2.41	SR23				
H12-13	NGC 300	00 55 04.01	−37 41 52.26	4.86	SR23	2.33	SR23				
H6-3	NGC 300	00 55 04.25	−37 40 52.20	> 4.77	SR23	3.27	SR23				
L5-8	NGC 300	00 55 07.22	−37 40 44.58	> 4.91	SR23	2.29	SR23				
PN 14	NGC 3109	10 03 10.34	−26 08 06.10					[WR]	PS07		
Hui93_2502	NGC 5128	13 24 03.36	−43 13 10.60	5.00	t.w.	3.29	t.w.				
P04_ctr804	NGC 5128	13 24 03.67	−43 17 51.50	4.62	t.w.	2.86	t.w.				
Hui93_2503	NGC 5128	13 24 07.24	−43 14 23.10	4.80	t.w.	3.13	t.w.				
EMMI_581	NGC 5128	13 24 07.25	−42 58 13.50	4.77	t.w.	3.08	t.w.				
P04_2701	NGC 5128	13 24 10.16	−43 21 11.00	4.78	t.w.	3.29	t.w.				
EMMI_580	NGC 5128	13 24 10.44	−42 57 03.10	4.89	t.w.	3.27	t.w.				
Hui93_2206	NGC 5128	13 24 15.38	−43 15 26.10	4.93	t.w.	3.10	t.w.				
Hui93_2703	NGC 5128	13 24 17.16	−43 19 27.50	4.78	t.w.	2.87	t.w.				
Hui93_2207	NGC 5128	13 24 20.10	−43 16 10.10	4.88	t.w.	2.91	t.w.				
EMMI_590	NGC 5128	13 24 21.26	−43 01 29.50	4.80	t.w.	3.01	t.w.				
Hui93_4805	NGC 5128	13 24 21.77	−42 59 28.60	4.95	t.w.	3.25	t.w.				
Hui93_2102	NGC 5128	13 24 22.28	−43 17 28.80	4.68	t.w.	2.93	t.w.				
Hui93_4807	NGC 5128	13 24 22.61	−42 58 49.80	4.94	t.w.	3.23	t.w.				
Hui93_2208	NGC 5128	13 24 22.92	−43 16 38.10	5.04	t.w.	3.14	t.w.				
Hui93_2901	NGC 5128	13 24 27.52	−43 14 26.30	4.71	t.w.	2.70	t.w.				
EMMI_552	NGC 5128	13 24 27.59	−43 03 23.20	4.53	t.w.	2.93	t.w.				
Hui93_2601	NGC 5128	13 24 27.66	−43 15 56.60	5.08	t.w.	3.35	t.w.				
Hui93_3501	NGC 5128	13 24 27.84	−43 10 12.30	5.09	t.w.	3.45	t.w.				
EMMI_542	NGC 5128	13 24 28.89	−43 00 13.80	5.32	t.w.	3.64	t.w.				
EMMI_575	NGC 5128	13 24 29.25	−43 05 41.50	5.15	t.w.	2.79	t.w.				
Hui93_2602	NGC 5128	13 24 29.35	−43 16 06.70	5.09	t.w.	3.21	t.w.				
P04_4702	NGC 5128	13 24 32.32	−42 55 42.80	4.73	t.w.	3.19	t.w.				
EMMI_1859	NGC 5128	13 24 32.69	−43 07 53.40	5.35	t.w.	3.23	t.w.				

Continued on next page

Table A.1 – continued.

Name	galaxy	RA_{J2000}	DEC_{J2000}	log T_{eff}	Ref.	$\log(L/L_\odot)$	Ref.	SpT	Ref.	RB	comm.
Hui93_4806	NGC 5128	13 24 32.75	−43 01 05.10	4.91	t.w.	3.22	t.w.				
EMMI_1829	NGC 5128	13 24 33.13	−43 02 30.10	4.58	t.w.	2.91	t.w.				
Hui93_2704	NGC 5128	13 24 33.97	−43 19 05.40	5.35	t.w.	3.42	t.w.				
EMMI_1857	NGC 5128	13 24 34.38	−43 06 55.90	4.85	t.w.	2.77	t.w.				
Hui93_3502	NGC 5128	13 24 34.53	−43 09 37.00	5.29	t.w.	2.97	t.w.				
EMMI_1830	NGC 5128	13 24 34.60	−43 03 02.10	5.00	t.w.	3.24	t.w.				
Hui93_3503	NGC 5128	13 24 35.22	−43 09 09.10	4.50	t.w.	3.23	t.w.				
Hui93_4804	NGC 5128	13 24 36.35	−43 00 38.50	5.57	t.w.	3.18	t.w.				
EMMI_541	NGC 5128	13 24 36.86	−42 59 46.60	4.81	t.w.	2.90	t.w.				
EMMI_1838	NGC 5128	13 24 37.01	−43 04 40.10	4.90	t.w.	3.45	t.w.				
Hui93_2603	NGC 5128	13 24 37.62	−43 16 09.80	4.86	t.w.	3.04	t.w.				
Hui93_4519	NGC 5128	13 24 38.41	−43 05 10.80	5.09	t.w.	3.24	t.w.				
Hui93_3402	NGC 5128	13 24 39.80	−43 12 32.50	6.09	t.w.	3.25	t.w.	[WR]?	t.w.		
P04_4803	NGC 5128	13 24 39.88	−42 59 11.00	5.10	t.w.	3.36	t.w.				
P04_2302	NGC 5128	13 24 40.39	−43 18 39.20	5.22	t.w.	2.98	t.w.				
EMMI_1862	NGC 5128	13 24 41.04	−43 08 21.50	4.65	t.w.	3.04	t.w.				
Hui93_2606	NGC 5128	13 24 42.34	−43 16 28.90	5.17	t.w.	3.39	t.w.				
Hui93_3504	NGC 5128	13 24 42.92	−43 11 18.20	5.07	t.w.	3.19	t.w.				
EMMI_476	NGC 5128	13 24 43.66	−42 58 29.30	5.02	t.w.	3.43	t.w.				
Hui93_4701	NGC 5128	13 24 44.21	−42 57 02.30	5.08	t.w.	3.49	t.w.				
Hui93_4515	NGC 5128	13 24 45.57	−43 01 37.40	4.96	t.w.	3.24	t.w.				
Hui93_3505	NGC 5128	13 24 45.87	−43 11 30.00	4.99	t.w.	3.20	t.w.				
EMMI_482	NGC 5128	13 24 46.84	−42 58 40.60	5.10	t.w.	3.58	t.w.				
Hui93_4507	NGC 5128	13 24 46.87	−43 03 31.50	4.84	t.w.	3.41	t.w.				
Hui93_2607	NGC 5128	13 24 46.91	−43 15 27.20	5.00	t.w.	3.16	t.w.				
Hui93_4503	NGC 5128	13 24 47.54	−43 04 12.50	5.00	t.w.	3.48	t.w.				
Hui93_3403	NGC 5128	13 24 48.17	−43 14 18.00	5.29	t.w.	3.49	t.w.				
Hui93_4514	NGC 5128	13 24 48.82	−43 04 16.20	5.17	t.w.	3.27	t.w.				
Hui93_3405	NGC 5128	13 24 48.96	−43 12 29.30	4.90	t.w.	2.93	t.w.				
EMMI_480	NGC 5128	13 24 49.00	−42 58 36.00	5.63	t.w.	3.37	t.w.	[WR]?	t.w.		
Hui93_4501	NGC 5128	13 24 49.08	−43 03 54.40	4.97	t.w.	3.50	t.w.				
P04_ctr703	NGC 5128	13 24 49.42	−42 57 32.50	4.81	t.w.	2.98	t.w.				
EMMI_500	NGC 5128	13 24 49.62	−43 00 42.40	4.75	t.w.	3.04	t.w.				
P04_4608	NGC 5128	13 24 49.88	−42 52 46.50	5.18	t.w.	3.31	t.w.				
Hui93_4518	NGC 5128	13 24 50.61	−43 03 43.30	4.72	t.w.	3.21	t.w.				
EMMI_491	NGC 5128	13 24 51.10	−43 00 08.80	5.45	t.w.	3.26	t.w.				
Hui93_4537	NGC 5128	13 24 51.37	−43 04 46.80	4.61	t.w.	2.73	t.w.				
EMMI_1766	NGC 5128	13 24 51.72	−43 01 05.40	4.65	t.w.	2.93	t.w.				
Hui93_4504	NGC 5128	13 24 51.81	−43 02 32.10	4.73	t.w.	3.46	t.w.				
EMMI_1812	NGC 5128	13 24 52.01	−43 07 26.20	4.83	t.w.	3.42	t.w.				
EMMI_1775	NGC 5128	13 24 52.09	−43 01 53.50	4.85	t.w.	3.22	t.w.				
Hui93_2306	NGC 5128	13 24 52.33	−43 18 38.30	5.01	t.w.	3.27	t.w.				
Hui93_4528	NGC 5128	13 24 52.50	−43 04 46.00	5.07	t.w.	3.05	t.w.				
Hui93_3508	NGC 5128	13 24 52.56	−43 10 00.20	5.18	t.w.	3.13	t.w.				
Hui93_4601	NGC 5128	13 24 52.65	−42 56 13.00	5.24	t.w.	3.60	t.w.				
P04_ctr622	NGC 5128	13 24 53.27	−42 53 26.50	4.62	t.w.	2.62	t.w.				
Hui93_4517	NGC 5128	13 24 53.38	−43 04 57.30	4.75	t.w.	3.24	t.w.				
EMMI_1818	NGC 5128	13 24 53.67	−43 09 50.00	5.05	t.w.	3.37	t.w.				
EMMI_1805	NGC 5128	13 24 53.69	−43 05 33.50	5.12	t.w.	3.45	t.w.				

Continued on next page

Table A.1 – continued.

Name	galaxy	RA_{J2000}	DEC_{J2000}	log T_{eff}	Ref.	log($L/L_\odot$)	Ref.	SpT	Ref.	RB	comm.
EMMI_405	NGC 5128	13 24 53.73	−42 56 58.00	5.22	t.w.	3.47	t.w.				
Hui93_4508	NGC 5128	13 24 54.10	−43 03 37.20	5.07	t.w.	3.40	t.w.				
Hui93_4502	NGC 5128	13 24 54.61	−43 02 18.50	5.13	t.w.	3.48	t.w.				
EMMI_1809	NGC 5128	13 24 54.73	−43 06 37.50	5.20	t.w.	3.25	t.w.				
Hui93_4422	NGC 5128	13 24 54.75	−42 58 49.70	5.05	t.w.	3.15	t.w.				
Hui93_4524	NGC 5128	13 24 54.94	−43 03 06.00	4.79	t.w.	3.12	t.w.				
Hui93_4533	NGC 5128	13 24 55.08	−43 03 21.60	4.71	t.w.	2.85	t.w.				
EMMI_418	NGC 5128	13 24 55.09	−42 59 10.60	4.74	t.w.	2.96	t.w.				
Hui93_4610	NGC 5128	13 24 55.83	−42 53 34.10	4.68	t.w.	3.11	t.w.				
Hui93_4527	NGC 5128	13 24 56.15	−43 03 13.20	4.69	t.w.	3.06	t.w.				
Hui93_4424	NGC 5128	13 24 56.75	−42 57 21.40	4.81	t.w.	3.07	t.w.				
EMMI_1771	NGC 5128	13 24 56.89	−43 01 23.60	5.34	t.w.	3.39	t.w.				
Hui93_4510	NGC 5128	13 24 57.18	−43 02 57.20	4.95	t.w.	3.35	t.w.				
P04_4609	NGC 5128	13 24 57.19	−42 56 10.20	5.62	t.w.	3.24	t.w.	[WR]?	t.w.		
Hui93_4520	NGC 5128	13 24 57.25	−43 03 05.00	4.80	t.w.	3.17	t.w.				
P04_4605	NGC 5128	13 24 57.60	−42 54 11.30	5.06	t.w.	3.40	t.w.				
Hui93_4538	NGC 5128	13 24 57.67	−43 03 31.20	4.55	t.w.	2.67	t.w.				
EMMI_430	NGC 5128	13 24 57.72	−43 00 56.30	5.02	t.w.	3.37	t.w.				
EMMI_1815	NGC 5128	13 24 57.76	−43 09 18.20	4.71	t.w.	2.89	t.w.				
Hui93_4511	NGC 5128	13 24 57.92	−43 04 07.50	4.96	t.w.	3.35	t.w.				
Hui93_4516	NGC 5128	13 24 57.98	−43 02 47.40	4.81	t.w.	3.31	t.w.				
EMMI_1767	NGC 5128	13 24 58.13	−43 01 06.70	5.29	t.w.	3.39	t.w.				
EMMI_429	NGC 5128	13 24 58.44	−43 00 56.70	4.68	t.w.	3.05	t.w.				
Hui93_4506	NGC 5128	13 24 58.59	−43 02 26.50	4.77	t.w.	3.38	t.w.				
Hui93_4413	NGC 5128	13 24 58.67	−42 57 39.20	4.83	t.w.	3.37	t.w.				
EMMI_427	NGC 5128	13 24 58.71	−43 00 33.70	5.11	t.w.	3.23	t.w.				
Hui93_4314	NGC 5128	13 24 58.86	−43 08 16.10	4.94	t.w.	3.33	t.w.				
Hui93_3001	NGC 5128	13 24 58.98	−43 16 33.00	5.37	t.w.	3.35	t.w.				
P04_4614	NGC 5128	13 24 59.26	−42 55 46.40	4.83	t.w.	2.94	t.w.				
Hui93_4604	NGC 5128	13 24 59.36	−42 55 33.30	4.88	t.w.	3.41	t.w.				
Hui93_4416	NGC 5128	13 24 59.40	−42 59 30.60	4.82	t.w.	3.29	t.w.				
P04_4421	NGC 5128	13 24 59.47	−42 59 43.60	4.73	t.w.	3.20	t.w.				
P04_4423	NGC 5128	13 24 59.61	−42 59 22.10	5.00	t.w.	3.14	t.w.				
Hui93_4612	NGC 5128	13 25 00.31	−42 55 48.20	4.90	t.w.	3.03	t.w.				
Hui93_3003	NGC 5128	13 25 00.76	−43 16 20.00	5.03	t.w.	3.33	t.w.				
EMMI_1769	NGC 5128	13 25 01.03	−43 01 10.50	5.68	t.w.	3.47	t.w.	[WR]?	t.w.		
EMMI_1774	NGC 5128	13 25 01.33	−43 01 50.10	4.76	t.w.	3.16	t.w.				
EMMI_316	NGC 5128	13 25 01.91	−42 57 16.90	5.34	t.w.	3.49	t.w.				
Hui93_4414	NGC 5128	13 25 02.17	−42 59 29.90	4.96	t.w.	3.46	t.w.				
Hui93_530	NGC 5128	13 25 02.25	−43 01 41.20	4.86	t.w.	3.25	t.w.				
EMMI_2350	NGC 5128	13 25 02.47	−43 08 58.50	4.86	t.w.	3.19	t.w.				
EMMI_1543	NGC 5128	13 25 02.69	−43 01 03.50	4.91	t.w.	3.41	t.w.				
Hui93_4307	NGC 5128	13 25 02.87	−43 09 39.60	4.96	t.w.	3.38	t.w.				
Hui93_4415	NGC 5128	13 25 02.91	−42 59 38.10	4.96	t.w.	3.31	t.w.				
Hui93_4313	NGC 5128	13 25 03.27	−43 06 49.90	4.90	t.w.	3.37	t.w.				
Hui93_4407	NGC 5128	13 25 03.62	−42 57 16.40	5.38	t.w.	3.53	t.w.				
EMMI_1698	NGC 5128	13 25 03.89	−43 03 43.30	5.17	t.w.	3.67	t.w.				
EMMI_326	NGC 5128	13 25 04.14	−42 59 03.50	4.67	t.w.	3.25	t.w.				
EMMI_1712	NGC 5128	13 25 04.30	−43 04 43.90	5.09	t.w.	3.51	t.w.				

Continued on next page

Table A.1 – continued.

Name	galaxy	RA_{J2000}	DEC_{J2000}	log T_{eff}	Ref.	log($L/L_{\odot}$)	Ref.	SpT	Ref.	RB	comm.
Hui93_511	NGC 5128	13 25 04.31	−43 01 11.30	4.88	t.w.	3.35	t.w.				
Hui93_4602	NGC 5128	13 25 04.38	−42 56 04.40	5.21	t.w.	3.55	t.w.				
EMMI_1730	NGC 5128	13 25 04.49	−43 05 31.70	5.14	t.w.	2.78	t.w.				
Hui93_519	NGC 5128	13 25 04.55	−43 02 29.00	5.20	t.w.	3.19	t.w.				
Hui93_4302	NGC 5128	13 25 04.72	−43 07 01.90	5.33	t.w.	3.51	t.w.				
EMMI_1697	NGC 5128	13 25 05.13	−43 03 43.10	4.84	t.w.	2.95	t.w.				
P04_541	NGC 5128	13 25 05.38	−43 01 08.10	5.42	t.w.	2.99	t.w.				
Hui93_537	NGC 5128	13 25 05.45	−43 01 29.90	5.14	t.w.	3.09	t.w.				
EMMI_318	NGC 5128	13 25 05.51	−42 58 11.20	5.89	t.w.	3.19	t.w.	[WR]?	t.w.		
EMMI_2357	NGC 5128	13 25 05.66	−43 09 51.70	4.89	t.w.	3.22	t.w.				
Hui93_4237	NGC 5128	13 25 05.94	−43 02 30.80	4.85	t.w.	3.26	t.w.				
Hui93_4275	NGC 5128	13 25 06.13	−43 05 41.20	4.72	t.w.	3.13	t.w.				
Hui93_4607	NGC 5128	13 25 06.56	−42 52 56.30	4.76	t.w.	3.29	t.w.				
P04_4430	NGC 5128	13 25 06.68	−42 58 16.20	4.78	t.w.	3.03	t.w.				
Hui93_4217	NGC 5128	13 25 06.72	−43 03 06.70	5.06	t.w.	3.44	t.w.				
Hui93_4412	NGC 5128	13 25 06.75	−42 58 58.70	5.29	t.w.	3.37	t.w.				
Hui93_4218	NGC 5128	13 25 06.82	−43 04 54.70	5.65	t.w.	3.43	t.w.	[WR]?	t.w.		
Hui93_513	NGC 5128	13 25 06.86	−43 01 19.00	4.82	t.w.	3.22	t.w.				
Hui93_4233	NGC 5128	13 25 07.11	−43 02 23.10	5.04	t.w.	3.23	t.w.				
Hui93_4606	NGC 5128	13 25 07.39	−42 53 11.50	5.07	t.w.	3.37	t.w.				
EMMI_2367	NGC 5128	13 25 07.55	−43 14 33.00	5.04	t.w.	3.59	t.w.				
Hui93_4312	NGC 5128	13 25 07.61	−43 07 38.10	4.83	t.w.	3.36	t.w.				
Hui93_4301	NGC 5128	13 25 07.98	−43 07 39.10	5.18	t.w.	3.70	t.w.				
EMMI_355	NGC 5128	13 25 08.96	−43 00 45.80	4.87	t.w.	3.33	t.w.				
Hui93_4411	NGC 5128	13 25 09.18	−42 59 08.40	4.88	t.w.	3.41	t.w.				
EMMI_2359	NGC 5128	13 25 09.29	−43 11 09.30	4.96	t.w.	3.16	t.w.				
EMMI_320	NGC 5128	13 25 09.35	−42 58 25.10	5.40	t.w.	3.10	t.w.				
Hui93_4229	NGC 5128	13 25 09.44	−43 05 25.90	4.81	t.w.	3.30	t.w.				
Hui93_42122	NGC 5128	13 25 09.54	−43 03 54.70	5.09	t.w.	2.77	t.w.				
Hui93_4603	NGC 5128	13 25 09.70	−42 55 04.80	5.15	t.w.	3.47	t.w.				
EMMI_333	NGC 5128	13 25 09.79	−42 59 29.00	4.51	t.w.	3.50	t.w.				
Hui93_4409	NGC 5128	13 25 10.53	−42 58 23.80	5.22	t.w.	3.46	t.w.				
Hui93_4308	NGC 5128	13 25 10.55	−43 09 26.20	4.80	t.w.	3.39	t.w.				
Hui93_528	NGC 5128	13 25 10.61	−43 00 30.20	4.74	t.w.	3.12	t.w.				
Hui93_4219	NGC 5128	13 25 10.81	−43 03 51.90	5.01	t.w.	3.36	t.w.				
Hui93_4305	NGC 5128	13 25 10.89	−43 09 48.30	4.92	t.w.	3.36	t.w.				
Hui93_4319	NGC 5128	13 25 10.90	−43 07 14.30	4.86	t.w.	3.07	t.w.				
EMMI_2360	NGC 5128	13 25 11.51	−43 12 07.80	4.64	t.w.	2.86	t.w.				
EMMI_1700	NGC 5128	13 25 11.51	−43 03 49.60	4.92	t.w.	3.16	t.w.				
Hui93_4420	NGC 5128	13 25 11.54	−43 00 04.40	5.17	t.w.	3.17	t.w.				
Hui93_4426	NGC 5128	13 25 11.76	−43 00 02.20	4.67	t.w.	3.11	t.w.				
EMMI_335	NGC 5128	13 25 12.13	−42 59 29.40	4.49	t.w.	3.49	t.w.				
EMMI_321	NGC 5128	13 25 12.33	−42 58 53.50	4.78	t.w.	2.81	t.w.				
Hui93_503	NGC 5128	13 25 12.39	−43 00 24.60	5.20	t.w.	3.28	t.w.				
Hui93_516	NGC 5128	13 25 12.55	−43 00 52.40	4.95	t.w.	3.20	t.w.				
Hui93_509	NGC 5128	13 25 12.58	−43 01 59.60	4.90	t.w.	3.38	t.w.				
Hui93_4323	NGC 5128	13 25 12.85	−43 06 47.30	4.72	t.w.	2.87	t.w.				
Hui93_4297	NGC 5128	13 25 13.03	−43 03 48.50	4.83	t.w.	2.95	t.w.				
Hui93_4246	NGC 5128	13 25 13.13	−43 02 14.20	4.99	t.w.	3.24	t.w.				

Continued on next page

Table A.1 – continued.

Name	galaxy	RA_{J2000}	DEC_{J2000}	log T_{eff}	Ref.	log($L/L_{\odot}$)	Ref.	SpT	Ref.	RB	comm.
Hui93_42126	NGC 5128	13 25 13.32	−43 04 49.10	4.73	t.w.	2.71	t.w.				
Hui93_4256	NGC 5128	13 25 13.32	−43 05 02.20	4.77	t.w.	3.19	t.w.				
EMMI_1515	NGC 5128	13 25 13.39	−43 05 40.20	4.55	t.w.	3.03	t.w.				
P04_1001	NGC 5128	13 25 13.56	−42 50 27.10	5.35	t.w.	3.47	t.w.				
Hui93_4295	NGC 5128	13 25 13.65	−43 03 31.90	5.21	t.w.	2.98	t.w.				
Hui93_4216	NGC 5128	13 25 13.75	−43 04 29.90	5.24	t.w.	3.37	t.w.				
EMMI_1717	NGC 5128	13 25 14.23	−43 04 54.30	5.23	t.w.	3.46	t.w.				
EMMI_314	NGC 5128	13 25 15.15	−42 56 49.10	5.46	t.w.	3.45	t.w.				
EMMI_1679	NGC 5128	13 25 15.18	−43 02 51.70	5.18	t.w.	3.22	t.w.				
Hui93_4231	NGC 5128	13 25 15.26	−43 02 47.40	5.81	t.w.	3.33	t.w.	[WR]?	t.w.		
Hui93_4214	NGC 5128	13 25 15.35	−43 03 02.40	5.09	t.w.	3.41	t.w.				
Hui93_42118	NGC 5128	13 25 15.54	−43 02 40.30	4.54	t.w.	2.99	t.w.				
Hui93_4257	NGC 5128	13 25 15.58	−43 03 57.90	4.85	t.w.	3.05	t.w.				
Hui93_4223	NGC 5128	13 25 15.61	−43 02 25.40	4.87	t.w.	3.53	t.w.				
EMMI_277	NGC 5128	13 25 16.07	−43 00 08.60	4.45	t.w.	3.78	t.w.				
Hui93_904	NGC 5128	13 25 16.17	−42 52 32.30	4.94	t.w.	3.41	t.w.				
Hui93_4241	NGC 5128	13 25 16.23	−43 05 11.30	4.77	t.w.	3.18	t.w.				
Hui93_526	NGC 5128	13 25 16.33	−43 00 20.30	4.65	t.w.	3.15	t.w.				
EMMI_280	NGC 5128	13 25 16.36	−43 00 13.10	4.53	t.w.	3.83	t.w.				
EMMI_1705	NGC 5128	13 25 16.49	−43 04 02.50	5.01	t.w.	3.66	t.w.				
Hui93_518	NGC 5128	13 25 16.56	−43 01 27.70	4.51	t.w.	3.19	t.w.				
Hui93_4280	NGC 5128	13 25 16.64	−43 03 50.50	4.83	t.w.	3.11	t.w.				
Hui93_4304	NGC 5128	13 25 16.64	−43 07 08.30	5.08	t.w.	3.43	t.w.				
Hui93_4306	NGC 5128	13 25 16.64	−43 07 48.40	5.45	t.w.	3.38	t.w.				
EMMI_1736	NGC 5128	13 25 16.65	−43 06 20.60	5.16	t.w.	3.48	t.w.				
EMMI_1031	NGC 5128	13 25 16.72	−42 56 57.00	4.82	t.w.	3.15	t.w.				
EMMI_1018	NGC 5128	13 25 16.82	−42 55 25.90	4.83	t.w.	3.11	t.w.				
Hui93_4222	NGC 5128	13 25 16.89	−43 04 11.20	4.93	t.w.	3.36	t.w.				
EMMI_1760	NGC 5128	13 25 17.02	−43 09 17.50	4.57	t.w.	3.23	t.w.				
P04_f18p24**	NGC 5128	13 25 17.12	−42 49 17.20	4.69	t.w.	3.19	t.w.				[17]
Hui93_4236	NGC 5128	13 25 17.13	−43 03 40.90	4.96	t.w.	3.28	t.w.				
EMMI_1100	NGC 5128	13 25 17.15	−43 00 26.30	4.49	t.w.	3.47	t.w.				
EMMI_1092	NGC 5128	13 25 17.28	−42 59 27.70	4.45	t.w.	3.27	t.w.				
EMMI_1026	NGC 5128	13 25 17.59	−42 56 33.20	4.81	t.w.	3.26	t.w.				
Hui93_4249	NGC 5128	13 25 17.68	−43 03 54.60	4.79	t.w.	3.27	t.w.				
EMMI_1044	NGC 5128	13 25 17.83	−42 57 56.90	4.96	t.w.	3.50	t.w.				
EMMI_1030	NGC 5128	13 25 17.87	−42 56 55.20	5.36	t.w.	3.67	t.w.				
Hui93_4315	NGC 5128	13 25 17.89	−43 08 05.60	5.08	t.w.	3.20	t.w.				
EMMI_1049	NGC 5128	13 25 17.90	−42 58 18.70	4.89	t.w.	3.21	t.w.				
Hui93_4311	NGC 5128	13 25 18.07	−43 08 43.70	4.99	t.w.	3.44	t.w.				
EMMI_1008	NGC 5128	13 25 18.52	−42 54 30.70	4.87	t.w.	3.21	t.w.				
EMMI_1097	NGC 5128	13 25 18.55	−42 59 47.70	4.45	t.w.	3.25	t.w.				
Hui93_4210	NGC 5128	13 25 18.56	−43 02 20.20	5.11	t.w.	3.65	t.w.				
Hui93_902	NGC 5128	13 25 18.80	−42 52 53.30	4.76	t.w.	3.52	t.w.				
EMMI_1110	NGC 5128	13 25 18.82	−43 01 33.30	4.54	t.w.	3.23	t.w.				
EMMI_1012	NGC 5128	13 25 18.82	−42 54 55.70	5.00	t.w.	3.25	t.w.				
EMMI_1107	NGC 5128	13 25 19.04	−43 01 20.90	4.45	t.w.	2.87	t.w.				
Hui93_4310	NGC 5128	13 25 19.52	−43 09 35.30	4.79	t.w.	3.35	t.w.				

Continued on next page

[17] full name: P04_f18p24_1003

Table A.1 – continued.

Name	galaxy	RA_{J2000}	DEC_{J2000}	log T_{eff}	Ref.	log($L/L_{\odot}$)	Ref.	SpT	Ref.	RB	comm.
EMMI_1053	NGC 5128	13 25 19.79	−42 58 23.10	4.84	t.w.	3.05	t.w.				
Hui93_4303	NGC 5128	13 25 19.84	−43 06 59.40	5.09	t.w.	3.58	t.w.				
Hui93_4201	NGC 5128	13 25 19.98	−43 05 28.70	5.20	t.w.	3.69	t.w.				
EMMI_1033	NGC 5128	13 25 20.01	−42 57 07.40	4.90	t.w.	3.16	t.w.				
Hui93_4272	NGC 5128	13 25 20.08	−43 02 21.70	5.11	t.w.	3.05	t.w.				
EMMI_1094	NGC 5128	13 25 20.25	−42 59 39.00	4.46	t.w.	3.24	t.w.				
EMMI_2303	NGC 5128	13 25 20.34	−43 07 49.70	4.68	t.w.	2.93	t.w.				
Hui93_4260	NGC 5128	13 25 20.53	−43 02 52.30	4.77	t.w.	3.04	t.w.				
EMMI_2295	NGC 5128	13 25 20.57	−43 06 49.50	5.04	t.w.	3.44	t.w.				
EMMI_1051	NGC 5128	13 25 21.16	−42 58 19.90	5.13	t.w.	3.49	t.w.				
Hui93_6101	NGC 5128	13 25 21.20	−43 10 04.70	5.03	t.w.	3.60	t.w.				
P04_4239	NGC 5128	13 25 21.23	−43 02 16.50	4.63	t.w.	3.20	t.w.				
EMMI_1052	NGC 5128	13 25 21.34	−42 58 21.20	4.96	t.w.	3.32	t.w.				
EMMI_1095	NGC 5128	13 25 21.44	−42 59 42.60	4.45	t.w.	2.97	t.w.				
EMMI_1002	NGC 5128	13 25 21.64	−42 53 25.10	5.16	t.w.	3.35	t.w.				
Hui93_4285	NGC 5128	13 25 21.75	−43 03 02.00	4.75	t.w.	3.08	t.w.				
Hui93_4202	NGC 5128	13 25 22.05	−43 03 20.50	5.35	t.w.	3.64	t.w.				
Hui93_4253	NGC 5128	13 25 22.19	−43 02 43.90	4.85	t.w.	3.17	t.w.				
Hui93_912	NGC 5128	13 25 22.21	−42 54 23.30	4.70	t.w.	3.14	t.w.				
EMMI_1041	NGC 5128	13 25 22.25	−42 57 52.20	4.91	t.w.	3.27	t.w.				
EMMI_1038	NGC 5128	13 25 22.47	−42 57 33.50	5.27	t.w.	3.64	t.w.				
Hui93_4206	NGC 5128	13 25 22.50	−43 03 21.00	5.11	t.w.	3.54	t.w.				
EMMI_1102	NGC 5128	13 25 22.56	−43 00 51.00	4.45	t.w.	3.24	t.w.				
EMMI_1495	NGC 5128	13 25 23.00	−43 03 45.10	5.03	t.w.	3.60	t.w.				
Hui93_4226	NGC 5128	13 25 23.01	−43 02 13.70	5.23	t.w.	3.35	t.w.				
Hui93_4207	NGC 5128	13 25 23.25	−43 02 49.60	5.08	t.w.	3.51	t.w.				
P04_4177	NGC 5128	13 25 23.29	−42 57 38.90	5.26	t.w.	3.01	t.w.				
Hui93_4145	NGC 5128	13 25 23.39	−42 57 28.40	4.89	t.w.	3.46	t.w.				
EMMI_2222	NGC 5128	13 25 23.69	−42 54 49.60	4.95	t.w.	3.22	t.w.				
Hui93_4228	NGC 5128	13 25 23.71	−43 03 29.50	5.13	t.w.	3.33	t.w.				
EMMI_1099	NGC 5128	13 25 23.91	−43 00 04.70	4.55	t.w.	3.66	t.w.				
Hui93_6103	NGC 5128	13 25 24.54	−43 09 14.10	5.48	t.w.	3.56	t.w.				
EMMI_1065	NGC 5128	13 25 24.81	−42 58 45.50	5.29	t.w.	3.46	t.w.				
EMMI_1337	NGC 5128	13 25 24.90	−43 06 21.10	4.91	t.w.	3.71	t.w.				
Hui93_4293	NGC 5128	13 25 25.03	−43 02 32.70	4.61	t.w.	2.96	t.w.				
Hui93_6102	NGC 5128	13 25 25.11	−43 10 41.20	5.04	t.w.	3.52	t.w.				
EMMI_2174	NGC 5128	13 25 25.14	−42 47 10.60	4.85	t.w.	2.65	t.w.				
Hui93_4113	NGC 5128	13 25 25.39	−42 58 54.60	5.08	t.w.	3.49	t.w.				
Hui93_4140	NGC 5128	13 25 25.66	−42 57 03.60	4.70	t.w.	3.36	t.w.				
Hui93_4121	NGC 5128	13 25 25.70	−42 58 19.60	4.92	t.w.	3.39	t.w.				
EMMI_2234	NGC 5128	13 25 25.73	−42 55 50.90	4.81	t.w.	2.95	t.w.				
EMMI_2200	NGC 5128	13 25 25.88	−42 52 09.50	4.86	t.w.	3.30	t.w.				
EMMI_1086	NGC 5128	13 25 26.33	−42 59 04.40	4.94	t.w.	3.27	t.w.				
Hui93_4264	NGC 5128	13 25 26.39	−43 03 54.10	4.89	t.w.	3.10	t.w.				
Hui93_4132	NGC 5128	13 25 26.61	−42 57 36.10	4.91	t.w.	3.23	t.w.				
Hui93_4130	NGC 5128	13 25 26.82	−42 58 30.90	4.86	t.w.	3.45	t.w.				
Hui93_4227	NGC 5128	13 25 26.83	−43 03 10.10	5.22	t.w.	3.12	t.w.				
Hui93_6118	NGC 5128	13 25 27.23	−43 09 39.00	4.72	t.w.	3.03	t.w.				

Continued on next page

Table A.1 – continued.

Name	galaxy	RA$_{J2000}$	DEC$_{J2000}$	log T$_{eff}$	Ref.	log(L/L$_\odot$)	Ref.	SpT	Ref.	RB	comm.
P04_f18p92**	NGC 5128	13 25 27.71	−42 50 57.10	4.89	t.w.	3.20	t.w.				[18]
Hui93_4119	NGC 5128	13 25 27.87	−42 58 47.30	4.97	t.w.	3.47	t.w.				
EMMI_2330	NGC 5128	13 25 27.87	−43 14 22.60	5.10	t.w.	3.56	t.w.				
Hui93_4108	NGC 5128	13 25 27.94	−42 58 03.50	4.97	t.w.	3.54	t.w.				
EMMI_1070	NGC 5128	13 25 27.97	−42 58 50.50	4.68	t.w.	3.20	t.w.				
Hui93_6108	NGC 5128	13 25 28.21	−43 07 54.60	4.79	t.w.	3.30	t.w.				
EMMI_2226	NGC 5128	13 25 28.26	−42 55 24.00	5.28	t.w.	3.65	t.w.				
Hui93_4144	NGC 5128	13 25 28.49	−42 59 22.60	5.06	t.w.	3.32	t.w.				
Hui93_6116	NGC 5128	13 25 28.67	−43 08 22.20	5.05	t.w.	2.98	t.w.				
EMMI_1408	NGC 5128	13 25 28.75	−43 04 47.00	4.83	t.w.	3.32	t.w.				
EMMI_1370	NGC 5128	13 25 28.85	−43 03 02.20	4.80	t.w.	2.81	t.w.				
Hui93_4105	NGC 5128	13 25 29.14	−42 59 01.40	5.14	t.w.	3.50	t.w.				
EMMI_2198	NGC 5128	13 25 29.21	−42 51 58.30	4.54	t.w.	2.65	t.w.				
EMMI_2296	NGC 5128	13 25 29.34	−43 06 50.80	5.11	t.w.	3.20	t.w.				
Hui93_4151	NGC 5128	13 25 29.45	−42 58 02.70	4.67	t.w.	3.21	t.w.				
EMMI_2221	NGC 5128	13 25 30.13	−42 54 48.10	5.18	t.w.	3.36	t.w.				
Hui93_6114	NGC 5128	13 25 30.35	−43 09 08.00	4.72	t.w.	3.02	t.w.				
EMMI_1075	NGC 5128	13 25 30.39	−42 58 51.40	4.96	t.w.	3.22	t.w.				
EMMI_1406	NGC 5128	13 25 30.86	−43 04 21.80	4.94	t.w.	3.04	t.w.				
Hui93_6106	NGC 5128	13 25 31.01	−43 10 12.10	4.71	t.w.	3.36	t.w.				
Hui93_6111	NGC 5128	13 25 31.01	−43 09 54.70	5.45	t.w.	3.28	t.w.				
EMMI_1382	NGC 5128	13 25 31.35	−43 03 32.50	5.08	t.w.	3.28	t.w.				
EMMI_1353	NGC 5128	13 25 31.47	−43 01 20.60	4.48	t.w.	2.69	t.w.				
EMMI_1411	NGC 5128	13 25 31.69	−43 05 02.00	4.87	t.w.	3.70	t.w.				
EMMI_1061	NGC 5128	13 25 31.72	−42 58 37.80	5.03	t.w.	3.48	t.w.				
P04_247	NGC 5128	13 25 32.39	−42 59 46.00	4.83	t.w.	2.99	t.w.				
P04_4127	NGC 5128	13 25 32.52	−42 57 50.70	4.59	t.w.	3.35	t.w.				
P04_4112	NGC 5128	13 25 32.70	−42 59 03.50	5.17	t.w.	3.52	t.w.				
EMMI_2199	NGC 5128	13 25 32.71	−42 52 01.40	4.64	t.w.	2.63	t.w.				
P04_906	NGC 5128	13 25 32.75	−42 54 05.90	5.05	t.w.	3.28	t.w.				
EMMI_2264	NGC 5128	13 25 32.93	−43 08 13.80	4.88	t.w.	3.16	t.w.				
Hui93_4103	NGC 5128	13 25 33.05	−42 57 15.20	5.28	t.w.	3.64	t.w.				
Hui93_4153	NGC 5128	13 25 33.29	−42 58 48.90	5.00	t.w.	3.15	t.w.				
Hui93_915	NGC 5128	13 25 33.48	−42 52 59.10	4.65	t.w.	2.86	t.w.				
EMMI_1390	NGC 5128	13 25 33.54	−43 03 55.50	4.90	t.w.	3.12	t.w.				
Hui93_4104	NGC 5128	13 25 33.82	−42 58 54.60	4.98	t.w.	3.59	t.w.				
Hui93_4126	NGC 5128	13 25 33.96	−43 00 02.90	4.96	t.w.	3.39	t.w.				
Hui93_4179	NGC 5128	13 25 34.00	−42 58 32.60	4.59	t.w.	2.91	t.w.				
EMMI_877	NGC 5128	13 25 34.27	−42 56 00.50	5.15	t.w.	3.41	t.w.				
EMMI_943	NGC 5128	13 25 34.36	−42 59 53.10	5.00	t.w.	3.22	t.w.				
Hui93_4107	NGC 5128	13 25 34.53	−42 58 26.70	4.90	t.w.	3.46	t.w.				
EMMI_2220	NGC 5128	13 25 34.58	−42 54 46.50	4.99	t.w.	3.01	t.w.				
Hui93_213	NGC 5128	13 25 34.62	−43 01 22.50	5.24	t.w.	3.35	t.w.				
EMMI_885	NGC 5128	13 25 34.75	−42 57 21.90	5.00	t.w.	3.12	t.w.				
EMMI_937	NGC 5128	13 25 34.80	−42 59 46.90	5.11	t.w.	3.13	t.w.				
EMMI_2223	NGC 5128	13 25 34.83	−42 55 13.60	4.78	t.w.	3.37	t.w.				
EMMI_2195	NGC 5128	13 25 34.87	−42 50 44.20	4.57	t.w.	2.58	t.w.				
EMMI_2259	NGC 5128	13 25 35.28	−43 06 01.40	4.98	t.w.	3.58	t.w.				

Continued on next page

[18] full name: P04_f18p92_1002

Table A.1 – continued.

Name	galaxy	RA_{J2000}	DEC_{J2000}	log T_{eff}	Ref.	log($L/L_\odot$)	Ref.	SpT	Ref.	RB	comm.
EMMI_921	NGC 5128	13 25 35.42	−42 59 13.40	4.67	t.w.	3.29	t.w.				
Hui93_239	NGC 5128	13 25 35.69	−43 00 40.90	5.01	t.w.	3.13	t.w.				
Hui93_6110	NGC 5128	13 25 35.85	−43 07 34.40	4.76	t.w.	3.18	t.w.				
Hui93_4142	NGC 5128	13 25 36.01	−42 59 44.80	4.89	t.w.	3.39	t.w.				
Hui93_4115	NGC 5128	13 25 36.07	−42 59 20.20	4.93	t.w.	3.54	t.w.				
Hui93_4110	NGC 5128	13 25 36.15	−42 59 44.10	4.90	t.w.	3.43	t.w.				
Hui93_4133	NGC 5128	13 25 36.18	−42 57 11.10	5.01	t.w.	3.30	t.w.				
EMMI_1402	NGC 5128	13 25 36.34	−43 04 13.40	4.90	t.w.	3.47	t.w.				
Hui93_4174	NGC 5128	13 25 36.37	−42 59 28.20	4.95	t.w.	3.10	t.w.				
Hui93_4131	NGC 5128	13 25 36.39	−42 59 18.10	4.71	t.w.	3.43	t.w.				
Hui93_4125	NGC 5128	13 25 36.39	−42 59 44.20	5.28	t.w.	3.32	t.w.				
EMMI_2194	NGC 5128	13 25 36.47	−42 50 27.20	4.90	t.w.	2.86	t.w.				
Hui93_4172	NGC 5128	13 25 36.60	−42 57 28.30	4.94	t.w.	3.23	t.w.				
EMMI_900	NGC 5128	13 25 36.64	−42 58 20.60	5.49	t.w.	3.41	t.w.				
EMMI_950	NGC 5128	13 25 36.67	−43 00 11.40	5.10	t.w.	3.38	t.w.				
Hui93_5434	NGC 5128	13 25 36.71	−43 05 15.10	5.06	t.w.	3.14	t.w.				
Hui93_212	NGC 5128	13 25 36.96	−43 00 59.30	4.97	t.w.	3.43	t.w.				
EMMI_1356	NGC 5128	13 25 37.28	−43 01 44.70	4.51	t.w.	3.45	t.w.				
Hui93_5422	NGC 5128	13 25 37.47	−43 03 38.60	4.83	t.w.	3.37	t.w.				
Hui93_245	NGC 5128	13 25 37.59	−43 00 32.90	4.80	t.w.	3.46	t.w.				
Hui93_1206	NGC 5128	13 25 37.63	−42 53 00.40	4.84	t.w.	3.52	t.w.				
Hui93_5417	NGC 5128	13 25 37.79	−43 04 07.20	5.38	t.w.	3.43	t.w.				
EMMI_942	NGC 5128	13 25 37.81	−42 59 53.30	4.99	t.w.	3.31	t.w.				
P04_4178	NGC 5128	13 25 37.87	−42 57 24.40	4.91	t.w.	3.01	t.w.				
EMMI_948	NGC 5128	13 25 37.94	−43 00 05.70	4.97	t.w.	3.25	t.w.				
Hui93_6104	NGC 5128	13 25 38.01	−43 07 01.70	4.98	t.w.	3.49	t.w.				
Hui93_1214	NGC 5128	13 25 38.04	−42 53 06.20	4.96	t.w.	3.14	t.w.				
EMMI_1198	NGC 5128	13 25 38.12	−43 02 03.30	4.46	t.w.	3.56	t.w.				
EMMI_933	NGC 5128	13 25 38.23	−42 59 39.70	5.36	t.w.	3.58	t.w.				
P04_201	NGC 5128	13 25 38.39	−43 00 52.40	5.27	t.w.	3.63	t.w.				
EMMI_889	NGC 5128	13 25 38.40	−42 57 35.80	5.02	t.w.	3.41	t.w.				
Hui93_4181	NGC 5128	13 25 38.57	−42 58 44.90	5.02	t.w.	3.01	t.w.				
P04_215	NGC 5128	13 25 39.09	−43 01 01.70	5.51	t.w.	3.35	t.w.				
EMMI_910	NGC 5128	13 25 39.38	−42 58 46.50	5.24	t.w.	3.38	t.w.				
Hui93_217	NGC 5128	13 25 39.53	−43 01 26.80	4.95	t.w.	3.33	t.w.				
Hui93_4124	NGC 5128	13 25 39.58	−42 58 33.90	5.23	t.w.	3.40	t.w.				
EMMI_929	NGC 5128	13 25 39.75	−42 59 34.50	5.22	t.w.	3.53	t.w.				
Hui93_4013	NGC 5128	13 25 40.91	−42 55 16.30	4.96	t.w.	3.33	t.w.				
P04_203	NGC 5128	13 25 40.92	−43 01 49.70	5.41	t.w.	3.57	t.w.				
Hui93_5428	NGC 5128	13 25 41.04	−43 03 32.90	5.27	t.w.	3.38	t.w.				
Hui93_4001	NGC 5128	13 25 41.18	−42 54 22.00	5.01	t.w.	3.58	t.w.				
P04_258	NGC 5128	13 25 41.34	−43 00 03.70	4.53	t.w.	2.82	t.w.				
EMMI_939	NGC 5128	13 25 41.36	−42 59 48.50	4.77	t.w.	3.33	t.w.				
Hui93_237	NGC 5128	13 25 41.61	−43 00 24.40	4.91	t.w.	3.14	t.w.				
EMMI_2164	NGC 5128	13 25 41.69	−42 56 24.80	4.58	t.w.	2.79	t.w.				
EMMI_922	NGC 5128	13 25 41.76	−42 59 17.20	5.14	t.w.	3.54	t.w.				
Hui93_5613	NGC 5128	13 25 41.83	−43 07 24.90	4.44	t.w.	3.19	t.w.				
Hui93_5454	NGC 5128	13 25 42.09	−43 03 27.80	4.69	t.w.	3.05	t.w.				
EMMI_913	NGC 5128	13 25 42.13	−42 58 56.40	5.29	t.w.	3.17	t.w.				

Continued on next page

Table A.1 – continued.

Name	galaxy	RA_{J2000}	DEC_{J2000}	log T_{eff}	Ref.	log($L/L_{\odot}$)	Ref.	SpT	Ref.	RB	comm.
Hui93_4117	NGC 5128	13 25 42.14	−42 57 52.80	4.90	t.w.	3.56	t.w.				
EMMI_904	NGC 5128	13 25 42.28	−42 58 31.50	4.59	t.w.	3.06	t.w.				
EMMI_2137	NGC 5128	13 25 42.32	−42 55 43.30	5.32	t.w.	3.30	t.w.				
Hui93_5430	NGC 5128	13 25 42.39	−43 03 45.40	4.71	t.w.	3.21	t.w.				
Hui93_202	NGC 5128	13 25 42.55	−43 01 07.40	5.26	t.w.	3.60	t.w.				
Hui93_256	NGC 5128	13 25 42.66	−43 00 48.00	4.79	t.w.	3.24	t.w.				
EMMI_1193	NGC 5128	13 25 43.08	−43 01 32.20	4.47	t.w.	2.85	t.w.				
Hui93_5421	NGC 5128	13 25 43.08	−43 04 27.40	4.88	t.w.	3.33	t.w.				
Hui93_5603	NGC 5128	13 25 43.12	−43 09 58.70	5.24	t.w.	3.34	t.w.				
Hui93_222	NGC 5128	13 25 43.32	−43 01 24.40	4.90	t.w.	3.25	t.w.				
P04_5617	NGC 5128	13 25 43.48	−43 10 25.80	5.01	t.w.	2.91	t.w.				
Hui93_4007	NGC 5128	13 25 43.80	−42 55 03.40	4.73	t.w.	3.37	t.w.				
EMMI_2100	NGC 5128	13 25 43.82	−42 51 40.60	4.78	t.w.	2.70	t.w.				
EMMI_903	NGC 5128	13 25 43.93	−42 58 28.60	5.00	t.w.	3.39	t.w.				
Hui93_5415	NGC 5128	13 25 44.06	−43 05 38.50	5.10	t.w.	3.40	t.w.				
Hui93_5612	NGC 5128	13 25 44.29	−43 09 54.70	4.82	t.w.	3.08	t.w.				
Hui93_5408	NGC 5128	13 25 44.39	−43 04 44.60	4.99	t.w.	3.48	t.w.				
EMMI_2283	NGC 5128	13 25 44.48	−43 13 46.40	4.98	t.w.	3.55	t.w.				
Hui93_5407	NGC 5128	13 25 44.59	−43 06 26.50	4.98	t.w.	3.48	t.w.				
EMMI_914	NGC 5128	13 25 44.59	−42 59 01.20	5.13	t.w.	3.54	t.w.				
EMMI_2096	NGC 5128	13 25 45.06	−42 50 19.30	5.18	t.w.	3.58	t.w.				
EMMI_901	NGC 5128	13 25 45.21	−42 58 21.60	4.89	t.w.	3.11	t.w.				
Hui93_5604	NGC 5128	13 25 45.34	−43 07 19.00	4.86	t.w.	3.26	t.w.				
Hui93_5429	NGC 5128	13 25 45.48	−43 03 22.80	4.78	t.w.	3.25	t.w.				
EMMI_2130	NGC 5128	13 25 45.89	−42 55 09.60	5.31	t.w.	2.69	t.w.				
Hui93_5413	NGC 5128	13 25 46.03	−43 04 52.90	5.04	t.w.	3.40	t.w.				
EMMI_2125	NGC 5128	13 25 46.12	−42 54 33.20	5.37	t.w.	3.51	t.w.				
Hui93_5409	NGC 5128	13 25 46.28	−43 05 46.50	5.00	t.w.	3.50	t.w.				
Hui93_1204	NGC 5128	13 25 46.36	−42 53 25.60	5.00	t.w.	3.46	t.w.				
Hui93_4025	NGC 5128	13 25 46.67	−42 57 38.30	5.03	t.w.	3.11	t.w.				
EMMI_886	NGC 5128	13 25 46.72	−42 57 27.10	4.85	t.w.	3.17	t.w.				
EMMI_920	NGC 5128	13 25 46.89	−42 59 10.30	4.66	t.w.	3.39	t.w.				
Hui93_221	NGC 5128	13 25 46.92	−43 00 38.70	4.73	t.w.	3.45	t.w.				
Hui93_5410	NGC 5128	13 25 47.34	−43 04 32.90	5.31	t.w.	3.47	t.w.				
Hui93_5439	NGC 5128	13 25 47.42	−43 03 40.30	4.74	t.w.	3.16	t.w.				
Hui93_4017	NGC 5128	13 25 47.72	−42 56 26.00	4.79	t.w.	3.20	t.w.				
EMMI_1253	NGC 5128	13 25 47.73	−43 05 09.30	4.72	t.w.	3.11	t.w.				
Hui93_4004	NGC 5128	13 25 47.73	−42 55 54.80	4.92	t.w.	3.47	t.w.				
Hui93_257	NGC 5128	13 25 47.87	−43 01 33.30	4.55	t.w.	3.11	t.w.				
Hui93_5418	NGC 5128	13 25 47.89	−43 05 12.30	4.96	t.w.	3.40	t.w.				
Hui93_207	NGC 5128	13 25 47.96	−43 00 00.70	5.02	t.w.	3.49	t.w.				
Hui93_1213	NGC 5128	13 25 48.35	−42 53 20.70	5.11	t.w.	3.09	t.w.				
EMMI_835	NGC 5128	13 25 48.61	−42 59 22.70	5.06	t.w.	3.50	t.w.				
Hui93_5450	NGC 5128	13 25 48.77	−43 05 59.50	4.65	t.w.	2.87	t.w.				
EMMI_815	NGC 5128	13 25 48.77	−42 57 08.20	5.14	t.w.	3.46	t.w.				
EMMI_812	NGC 5128	13 25 48.91	−42 56 54.10	5.17	t.w.	3.53	t.w.				
EMMI_829	NGC 5128	13 25 49.09	−42 58 36.30	4.71	t.w.	3.45	t.w.				
P04_5616	NGC 5128	13 25 49.63	−43 09 56.80	4.62	t.w.	2.99	t.w.				
EMMI_1258	NGC 5128	13 25 49.67	−43 05 48.90	5.00	t.w.	3.43	t.w.				

Continued on next page

Table A.1 – continued.

Name	galaxy	RA_{J2000}	DEC_{J2000}	log T_{eff}	Ref.	$\log(L/L_\odot)$	Ref.	SpT	Ref.	RB	comm.
Hui93_5444	NGC 5128	13 25 49.72	−43 03 06.20	5.07	t.w.	3.02	t.w.				
EMMI_826	NGC 5128	13 25 49.75	−42 58 11.10	4.85	t.w.	3.01	t.w.				
Hui93_5602	NGC 5128	13 25 50.25	−43 07 19.70	4.92	t.w.	3.48	t.w.				
Hui93_242	NGC 5128	13 25 50.49	−43 00 39.20	4.64	t.w.	3.05	t.w.				
Hui93_4020	NGC 5128	13 25 50.77	−42 55 50.60	4.75	t.w.	3.23	t.w.				
EMMI_832	NGC 5128	13 25 50.86	−42 58 57.50	5.02	t.w.	3.26	t.w.	[WR]?	t.w.		
EMMI_2138	NGC 5128	13 25 51.14	−42 55 48.20	4.88	t.w.	3.10	t.w.	[WR]?	t.w.		
EMMI_833	NGC 5128	13 25 51.41	−42 59 03.00	5.16	t.w.	3.44	t.w.				
Hui93_4012	NGC 5128	13 25 52.12	−42 56 11.30	4.80	t.w.	3.31	t.w.				
Hui93_4014	NGC 5128	13 25 52.36	−42 54 15.20	4.97	t.w.	3.31	t.w.				
Hui93_4016	NGC 5128	13 25 52.55	−42 57 21.80	5.02	t.w.	3.23	t.w.				
Hui93_5601	NGC 5128	13 25 53.58	−43 08 53.10	5.06	t.w.	3.66	t.w.				
EMMI_2132	NGC 5128	13 25 53.67	−42 55 19.00	4.82	t.w.	3.21	t.w.				
Hui93_4011	NGC 5128	13 25 53.79	−42 57 07.90	4.98	t.w.	3.33	t.w.				
Hui93_5621	NGC 5128	13 25 53.87	−43 08 35.90	4.90	t.w.	2.88	t.w.				
Hui93_5605	NGC 5128	13 25 53.93	−43 09 56.40	4.75	t.w.	3.23	t.w.				
EMMI_2058	NGC 5128	13 25 54.14	−42 52 05.90	4.70	t.w.	2.87	t.w.				
EMMI_1145	NGC 5128	13 25 54.14	−43 01 35.80	4.71	t.w.	3.26	t.w.				
Hui93_4006	NGC 5128	13 25 54.37	−42 57 23.70	5.24	t.w.	3.36	t.w.				
EMMI_2061	NGC 5128	13 25 54.63	−42 52 17.70	5.41	t.w.	3.46	t.w.				
EMMI_837	NGC 5128	13 25 54.74	−42 59 35.30	4.95	t.w.	3.25	t.w.				
EMMI_824	NGC 5128	13 25 54.81	−42 58 04.90	5.20	t.w.	2.86	t.w.				
Hui93_4008	NGC 5128	13 25 55.03	−42 55 48.50	4.81	t.w.	3.38	t.w.				
Hui93_5436	NGC 5128	13 25 55.35	−43 05 15.60	4.84	t.w.	2.99	t.w.				
EMMI_831	NGC 5128	13 25 55.68	−42 58 56.40	4.99	t.w.	3.46	t.w.				
EMMI_834	NGC 5128	13 25 56.25	−42 59 14.00	4.99	t.w.	2.94	t.w.				
EMMI_839	NGC 5128	13 25 56.49	−43 00 21.30	5.43	t.w.	3.35	t.w.				
Hui93_4028	NGC 5128	13 25 57.61	−42 57 21.90	4.71	t.w.	3.01	t.w.				
EMMI_842	NGC 5128	13 25 57.78	−43 00 41.10	4.73	t.w.	2.98	t.w.				
EMMI_1161	NGC 5128	13 25 58.84	−43 04 18.50	4.83	t.w.	2.82	t.w.				
EMMI_2514	NGC 5128	13 25 59.13	−42 45 46.70	5.26	t.w.	3.04	t.w.				
Hui93_5304	NGC 5128	13 25 59.58	−43 03 42.40	4.91	t.w.	3.26	t.w.				
EMMI_2508	NGC 5128	13 25 59.76	−42 44 07.60	5.30	t.w.	3.23	t.w.				
Hui93_4032	NGC 5128	13 25 59.87	−42 57 11.30	4.51	t.w.	2.79	t.w.				
Hui93_5504	NGC 5128	13 25 59.96	−43 06 15.70	4.88	t.w.	3.24	t.w.				
Hui93_5310	NGC 5128	13 26 00.25	−43 04 23.50	4.77	t.w.	3.12	t.w.				
EMMI_1156	NGC 5128	13 26 00.60	−43 03 20.80	4.82	t.w.	3.28	t.w.				
EMMI_2070	NGC 5128	13 26 00.72	−42 54 00.80	5.11	t.w.	3.44	t.w.				
EMMI_838	NGC 5128	13 26 00.75	−42 59 54.60	4.71	t.w.	3.06	t.w.				
EMMI_2053	NGC 5128	13 26 01.27	−42 50 21.70	4.83	t.w.	3.16	t.w.				
EMMI_825	NGC 5128	13 26 01.41	−42 58 05.20	4.69	t.w.	3.28	t.w.				
P04_5302	NGC 5128	13 26 01.81	−43 04 30.10	5.66	t.w.	3.41	t.w.	[WR]?	t.w.		
EMMI_760	NGC 5128	13 26 01.99	−42 57 58.40	4.67	t.w.	3.65	t.w.				
Hui93_5104	NGC 5128	13 26 02.13	−42 56 05.10	4.83	t.w.	3.33	t.w.				
EMMI_2044	NGC 5128	13 26 02.14	−42 48 50.40	4.79	t.w.	2.94	t.w.				
EMMI_2059	NGC 5128	13 26 02.24	−42 52 07.40	4.70	t.w.	2.99	t.w.				
EMMI_844	NGC 5128	13 26 02.29	−43 00 48.50	5.08	t.w.	3.28	t.w.				
Hui93_5501	NGC 5128	13 26 02.36	−43 06 42.20	5.02	t.w.	3.45	t.w.				
EMMI_1148	NGC 5128	13 26 02.36	−43 02 07.30	5.30	t.w.	3.44	t.w.				

Continued on next page

Table A.1 – continued.

Name	galaxy	RA_{J2000}	DEC_{J2000}	log T_{eff}	Ref.	log($L/L_{\odot}$)	Ref.	SpT	Ref.	RB	comm.
EMMI_2483	NGC 5128	13 26 02.41	−42 39 05.80	4.86	t.w.	3.01	t.w.				
EMMI_2042	NGC 5128	13 26 02.48	−42 47 53.30	4.80	t.w.	2.61	t.w.				
EMMI_2057	NGC 5128	13 26 02.59	−42 51 07.50	4.60	t.w.	2.95	t.w.				
Hui93_1217	NGC 5128	13 26 02.60	−42 53 06.90	4.62	t.w.	3.02	t.w.				
EMMI_758	NGC 5128	13 26 02.70	−42 57 52.20	4.71	t.w.	3.25	t.w.				
EMMI_847	NGC 5128	13 26 02.92	−43 00 57.40	5.16	t.w.	3.39	t.w.				
EMMI_2045	NGC 5128	13 26 03.89	−42 49 08.10	5.77	t.w.	3.24	t.w.	[WR]?	t.w.		
EMMI_2516	NGC 5128	13 26 04.00	−42 46 41.90	5.11	t.w.	3.36	t.w.				
EMMI_2047	NGC 5128	13 26 04.41	−42 49 29.50	4.75	t.w.	2.88	t.w.				
Hui93_1303	NGC 5128	13 26 05.40	−42 51 31.30	4.86	t.w.	3.35	t.w.				
EMMI_694	NGC 5128	13 26 05.69	−42 58 54.70	5.01	t.w.	3.26	t.w.				
Hui93_5117	NGC 5128	13 26 05.75	−42 55 18.90	4.68	t.w.	2.92	t.w.				
Hui93_5301	NGC 5128	13 26 05.80	−43 02 57.00	5.07	t.w.	3.60	t.w.				
EMMI_680	NGC 5128	13 26 05.98	−42 56 31.80	4.88	t.w.	3.00	t.w.				
EMMI_714	NGC 5128	13 26 06.02	−43 00 44.80	4.82	t.w.	3.11	t.w.				
EMMI_2075	NGC 5128	13 26 06.13	−42 54 49.30	4.81	t.w.	3.07	t.w.				
EMMI_681	NGC 5128	13 26 06.15	−42 56 33.50	4.78	t.w.	2.90	t.w.				
EMMI_690	NGC 5128	13 26 06.68	−42 57 44.50	5.08	t.w.	3.36	t.w.				
Hui93_5101	NGC 5128	13 26 07.37	−42 58 07.30	4.97	t.w.	3.50	t.w.				
EMMI_666	NGC 5128	13 26 07.42	−42 54 35.90	4.89	t.w.	2.90	t.w.				
Hui93_5105	NGC 5128	13 26 07.70	−42 55 53.50	5.00	t.w.	3.39	t.w.				
EMMI_93	NGC 5128	13 26 08.78	−42 56 24.60	4.93	t.w.	3.87	t.w.				
EMMI_98	NGC 5128	13 26 09.03	−43 00 40.80	5.03	t.w.	3.41	t.w.				
EMMI_1981	NGC 5128	13 26 09.40	−42 48 11.50	5.44	t.w.	3.45	t.w.				
P04_5505	NGC 5128	13 26 09.89	−43 06 13.90	5.70	t.w.	3.21	t.w.	[WR]?	t.w.		
EMMI_2029	NGC 5128	13 26 10.13	−42 54 31.00	4.75	t.w.	3.40	t.w.				
Hui93_5202	NGC 5128	13 26 10.30	−42 59 37.00	5.14	t.w.	3.63	t.w.				
EMMI_2024	NGC 5128	13 26 10.88	−42 54 01.20	4.75	t.w.	3.21	t.w.				
Hui93_5206	NGC 5128	13 26 11.08	−42 58 21.70	4.76	t.w.	3.16	t.w.				
EMMI_2033	NGC 5128	13 26 11.32	−42 55 38.30	4.62	t.w.	2.89	t.w.				
EMMI_2474	NGC 5128	13 26 11.35	−42 46 45.10	4.80	t.w.	3.06	t.w.				
Hui93_5106	NGC 5128	13 26 11.58	−42 55 37.40	4.78	t.w.	3.27	t.w.				
Hui93_5102	NGC 5128	13 26 11.83	−42 56 18.90	4.85	t.w.	3.45	t.w.				
EMMI_2025	NGC 5128	13 26 12.23	−42 54 02.90	4.45	t.w.	2.87	t.w.				
EMMI_100	NGC 5128	13 26 12.29	−43 01 16.90	4.74	t.w.	3.03	t.w.				
Hui93_5306	NGC 5128	13 26 12.53	−43 03 00.20	4.80	t.w.	3.21	t.w.				
EMMI_1993	NGC 5128	13 26 12.70	−42 49 36.30	4.76	t.w.	3.02	t.w.				
EMMI_2027	NGC 5128	13 26 12.77	−42 54 24.10	4.92	t.w.	3.16	t.w.				
Hui93_5309	NGC 5128	13 26 12.99	−43 03 43.30	4.80	t.w.	3.12	t.w.				
EMMI_686	NGC 5128	13 26 13.19	−42 57 22.40	4.87	t.w.	3.04	t.w.				
EMMI_2023	NGC 5128	13 26 13.52	−42 53 50.00	5.00	t.w.	2.87	t.w.				
EMMI_661	NGC 5128	13 26 13.74	−42 53 41.90	4.92	t.w.	2.97	t.w.				
EMMI_684	NGC 5128	13 26 13.80	−42 57 11.70	5.01	t.w.	3.14	t.w.				
EMMI_104	NGC 5128	13 26 14.56	−43 01 51.10	5.00	t.w.	3.43	t.w.				
Hui93_5213	NGC 5128	13 26 14.78	−42 58 58.50	4.76	t.w.	2.85	t.w.				
Hui93_5201	NGC 5128	13 26 15.19	−43 00 50.70	5.12	t.w.	3.69	t.w.				
EMMI_682	NGC 5128	13 26 15.31	−42 56 49.20	4.80	t.w.	2.86	t.w.				
EMMI_693	NGC 5128	13 26 17.28	−42 58 45.20	4.88	t.w.	3.03	t.w.				
EMMI_1988	NGC 5128	13 26 17.46	−42 49 17.70	4.96	t.w.	3.27	t.w.				

Continued on next page

Table A.1 – continued.

Name	galaxy	RA_{J2000}	DEC_{J2000}	log T_{eff}	Ref.	log($L/L_{\odot}$)	Ref.	SpT	Ref.	RB	comm.
P04_f17p19**	NGC 5128	13 26 18.05	−42 50 30.50	5.54	t.w.	3.49	t.w.				[19]
EMMI_63	NGC 5128	13 26 19.50	−42 56 53.70	4.70	t.w.	3.06	t.w.				
EMMI_2013	NGC 5128	13 26 19.69	−42 52 40.60	4.61	t.w.	2.97	t.w.				
EMMI_2005	NGC 5128	13 26 20.81	−42 51 47.50	4.51	t.w.	3.25	t.w.				
EMMI_90	NGC 5128	13 26 22.00	−43 04 51.30	4.93	t.w.	3.42	t.w.				
P04_5218	NGC 5128	13 26 22.22	−42 57 55.00	4.83	t.w.	2.59	t.w.	[WR]?	t.w.		
P04_5215	NGC 5128	13 26 22.38	−43 00 57.10	4.93	t.w.	2.69	t.w.				
EMMI_78	NGC 5128	13 26 22.96	−43 02 02.50	4.82	t.w.	2.67	t.w.				
EMMI_1910	NGC 5128	13 26 23.66	−42 48 08.10	5.49	t.w.	3.40	t.w.				
EMMI_1932	NGC 5128	13 26 25.25	−42 49 38.30	4.65	t.w.	3.76	t.w.				
EMMI_1953	NGC 5128	13 26 25.45	−42 54 16.90	4.76	t.w.	3.02	t.w.				
EMMI_1924	NGC 5128	13 26 25.57	−42 49 28.10	4.70	t.w.	3.22	t.w.				
P04_f18p34**	NGC 5128	13 26 25.86	−42 45 58.60	4.97	t.w.	3.55	t.w.				[20]
EMMI_2456	NGC 5128	13 26 26.20	−42 47 13.30	4.58	t.w.	3.09	t.w.				
EMMI_614	NGC 5128	13 26 26.30	−42 57 26.60	4.71	t.w.	3.23	t.w.				
Hui93_5203	NGC 5128	13 26 26.35	−43 00 37.30	5.06	t.w.	3.46	t.w.				
EMMI_1941	NGC 5128	13 26 27.91	−42 50 31.00	4.75	t.w.	2.81	t.w.				
EMMI_615	NGC 5128	13 26 28.82	−42 57 27.60	4.83	t.w.	3.11	t.w.				
EMMI_1920	NGC 5128	13 26 28.90	−42 49 06.30	4.57	t.w.	3.49	t.w.				
EMMI_2431	NGC 5128	13 26 29.39	−42 42 26.30	4.90	t.w.	3.38	t.w.				
EMMI_622	NGC 5128	13 26 29.43	−42 58 40.60	5.45	t.w.	3.22	t.w.				
P04_ctr602	NGC 5128	13 26 30.29	−42 45 16.00	4.79	t.w.	3.23	t.w.				
EMMI_1947	NGC 5128	13 26 30.62	−42 51 15.50	4.67	t.w.	2.71	t.w.				
EMMI_1936	NGC 5128	13 26 30.62	−42 49 54.90	4.74	t.w.	3.31	t.w.				
EMMI_41	NGC 5128	13 26 31.08	−43 02 33.60	5.01	t.w.	3.55	t.w.				
EMMI_1935	NGC 5128	13 26 31.37	−42 49 46.40	5.32	t.w.	3.16	t.w.	[WR]?	t.w.		
EMMI_1952	NGC 5128	13 26 32.94	−42 53 57.60	5.18	t.w.	3.57	t.w.				
EMMI_1922	NGC 5128	13 26 33.13	−42 49 16.40	4.67	t.w.	2.81	t.w.				
EMMI_1945	NGC 5128	13 26 34.59	−42 51 01.40	4.91	t.w.	3.22	t.w.				
EMMI_1948	NGC 5128	13 26 36.27	−42 51 33.40	4.94	t.w.	3.45	t.w.				
EMMI_2427	NGC 5128	13 26 38.40	−42 39 02.10	5.04	t.w.	3.17	t.w.				
EMMI_1898	NGC 5128	13 26 40.01	−42 55 56.50	4.96	t.w.	3.17	t.w.				
P04_1902	NGC 5128	13 26 40.84	−42 49 32.00	5.38	t.w.	3.53	t.w.				
EMMI_1888	NGC 5128	13 26 40.88	−42 52 38.30	4.83	t.w.	3.03	t.w.				
EMMI_59	NGC 5128	13 26 40.92	−43 05 04.10	5.06	t.w.	3.54	t.w.				
EMMI_49	NGC 5128	13 26 41.18	−43 04 11.40	5.03	t.w.	3.31	t.w.				
EMMI_2416	NGC 5128	13 26 42.77	−42 43 04.80	4.82	t.w.	2.72	t.w.				
EMMI_1887	NGC 5128	13 26 44.22	−42 52 29.90	4.80	t.w.	3.35	t.w.				
EMMI_1889	NGC 5128	13 26 45.99	−42 53 31.20	5.20	t.w.	3.16	t.w.				
EMMI_1882	NGC 5128	13 26 47.68	−42 51 34.50	4.55	t.w.	2.89	t.w.				
EMMI_1871	NGC 5128	13 26 47.79	−42 48 33.60	5.20	t.w.	3.50	t.w.				
EMMI_1884	NGC 5128	13 26 51.19	−42 51 49.80	4.87	t.w.	3.41	t.w.				
EMMI_4	NGC 5128	13 26 53.46	−42 58 03.30	4.77	t.w.	3.43	t.w.				
EMMI_1885	NGC 5128	13 26 53.50	−42 52 13.10	4.98	t.w.	3.61	t.w.				
EMMI_2380	NGC 5128	13 27 01.75	−42 40 00.60	4.87	t.w.	2.97	t.w.				
EMMI_2393	NGC 5128	13 27 01.75	−42 42 59.40	5.01	t.w.	3.11	t.w.				
EMMI_2394	NGC 5128	13 27 05.10	−42 43 18.90	5.24	t.w.	3.14	t.w.				

Continued on next page

[19] full name: P04_f17p19_1401
[20] full name: P04_f18p34_1601

Table A.1 – continued.

Name	galaxy	RA_{J2000}	DEC_{J2000}	log T_{eff}	Ref.	log($L/L_\odot$)	Ref.	SpT	Ref.	RB	comm.
NGC5236-254	NGC 5236	13 37 00.91	−29 51 56.74	4.66	LR06	3.79	LR06				[21]
NGC5236-487	NGC 5236	13 37 00.91	−29 51 56.74	4.65	LR06	3.73	LR06				[22]
Bennu	Phoenix	01 51 05.45	−44 26 55.28	5.08	SE09	3.41	SE09				
SexA-PN	Sextans A	10 11 01.58	−04 41 22.90	5.29	ML05	3.90	ML05				
SexB PN1	Sextans B	09 59 53.06	+05 18 52.10	4.79	ML05	3.50	ML05				
SexB PN2	Sextans B	09 59 56.50	+05 19 29.50	4.89	ML05	3.30	ML05				
SexB PN3	Sextans B	09 59 56.64	+05 19 52.60	4.86	ML05	3.50	ML05				
SexB PN4	Sextans B	10 00 00.19	+05 20 37.20	4.81	ML05	3.20	ML05				
SexB PN5	Sextans B	10 00 10.48	+05 20 31.90	4.95	ML05	3.60	ML05				
StWr 2-21	Sgr dSph	19 14 23.35	−32 34 16.96	5.08	ZG06	3.61	ZG06	[WO 2]	ZG06		
WRAY 16-423	Sgr dSph	19 22 10.63	−31 30 38.70	5.03	ZG06	3.64	ZG06	[WC 4] / WELS	ZG06		
Hen 2-436	Sgr dSph	19 32 06.71	−34 12 57.52	4.85	ZG06	3.73	ZG06	[WO 4] / [WC 4]	ZG06		
MGPN 1	SMC	00 23 32.80	−74 52 31.00	5.09	IM07	4.36	IM07				
SMP 1	SMC	00 23 58.67	−73 38 03.80	< 4.67	VS04	3.77	VS04			VS04	
MGPN 2	SMC	00 28 10.40	−72 58 44.63	5.00	IM07	5.13	IM07				
MGPN 3	SMC	00 29 21.00	−72 14 07.00	5.09	IM07	2.76	IM07				
SMP 2	SMC	00 32 39.00	−71 41 59.00	5.17	IM07	3.81	IM07				
SMP 3	SMC	00 34 21.00	−73 13 24.00	5.01	IM07	3.20	IM07				
SMP 4	SMC	00 40 42.00	−75 17 00.00	4.84	IM07	3.45	IM07				
SMP 13	SMC	00 40 51.71	−73 44 21.30	< 4.64	VS04	< 4.03	VS04				
SMP 5	SMC	00 41 22.00	−72 45 17.00	5.22	IM07	3.91	IM07				
MGPN 5	SMC	00 41 27.30	−75 02 52.00	5.50	IM07	2.71	IM07				
SMP 6	SMC	00 41 27.52	−73 47 06.20	< 4.64	VS04	3.86	VS04	[WC 4–5]	MB88	MB88	
SMP 7	SMC	00 42 28.00	−73 20 55.00	5.01	IM07	2.77	IM07				
SMP 8	SMC	00 43 25.17	−72 38 18.90	4.57	VS04	3.56	VS04	P-Cygni	SL09	SL09	
LIN 49	SMC	00 43 53.89	−72 55 14.79	4.48	OK16	3.77	OK16	O(H) 8-9	OK16		[23]
MGPN 6	SMC	00 44 25.72	−73 51 39.16	5.53	IM07	2.93	IM07				
SMP 9	SMC	00 45 20.66	−73 24 10.50	5.24	VS04	2.95	VS04			VS04	
J4	SMC	00 45 27.30	−73 42 15.30	4.87	VS04	4.17	VS04				
SMP 10	SMC	00 47 00.00	−72 49 16.00	4.84	IM07	3.77	IM07				
MGPN 7	SMC	00 47 42.50	−74 48 15.00	5.16	IM07	3.55	IM07				
SMP 11	SMC	00 48 36.61	−72 58 00.10	< 4.72	VS04	3.22	VS04				
SMP 12	SMC	00 49 21.00	−73 52 58.00	< 4.71	VS04	2.84	VS04				
SMP 14	SMC	00 50 34.99	−73 42 57.90	5.07	VS04	3.53	VS04			VS04	
SMP 15	SMC	00 51 07.38	−73 57 37.60	4.84	IM07	3.92	IM07	P-Cygni	SL09		
SMP 16	SMC	00 51 27.00	−72 26 11.00	4.84	IM07	3.47	IM07	P-Cygni	SL09		
J18	SMC	00 51 43.39	−73 00 54.10	4.72	VS04	3.33	VS04			VS04	
SMP 17	SMC	00 51 56.41	−71 24 44.60	< 4.77	VS04	3.65	VS04			VS04	
SMP 18	SMC	00 51 57.97	−73 20 30.10	4.50	VS04	3.85	VS04				
SMP 19	SMC	00 53 11.14	−72 45 07.50	5.00	VS04	< 3.90	VS04				
J23	SMC	00 55 30.52	−72 50 21.30	4.74	VS04	4.65	VS04	Broad Hα emission	SH03		
SMP 20	SMC	00 56 05.39	−70 19 24.70	< 4.77	VS04	3.71	VS04	P-Cygni	SL09		[24]
MGPN 8	SMC	00 56 19.59	−72 06 58.50	5.15	IM07	2.98	IM07	[WC 8]	MB88	MB88	
SMP 21	SMC	00 56 31.00	−72 27 01.00	5.20	IM07	3.28	IM07				

Continued on next page

[21] PN Candidate.
[22] PN Candidate.
[23] The authors do not give the spectral subtype. They only say that they fitted a model of O-type stars. We classify it as subtype O(H) 8 – 9.
[24] The stellar spectrum shows a feature at about 6577Å(SH03).

Table A.1 – continued.

Name	galaxy	RA_{J2000}	DEC_{J2000}	log T_{eff}	Ref.	log($L/L_{\odot}$)	Ref.	SpT	Ref.	RB	comm.
LIN 321	SMC	00 57 29.96	−72 32 24.00					O(H) V	HG14	HG14	[25]
SMP 22	SMC	00 58 37.44	−71 35 49.10	5.09	VS04	< 4.04	VS04				[26]
SMP 23	SMC	00 58 42.14	−72 56 59.60	4.79	VS04	3.61	VS04			VS04	
MGPN 9	SMC	00 58 42.86	−72 27 16.70	4.84	IM07						
SMP 24	SMC	00 59 16.09	−72 01 59.70	4.58	VS04	3.70	VS04			VS04	
J27	SMC	00 59 43.48	−72 57 17.90	4.96	VS04	< 1.63	VS04				
SMP 26	SMC	01 04 17.81	−73 21 51.20	5.05	VS04	< 3.41	VS04				
MGPN 10	SMC	01 04 51.12	−73 05 21.40	5.53	IM07	3.26	IM07				
MGPN 11	SMC	01 08 40.50	−72 18 08.74	3.88	IM07	2.00	IM07				
SMP 34	SMC	01 12 10.76	−71 26 50.20	4.90	VS04	< 2.87	VS04				
MGPN 12	SMC	01 14 23.97	−71 05 21.25	5.30	IM07						
SMP 27	SMC	01 21 10.67	−73 14 35.40	4.64	VS04	3.77	VS04			VS04	
SMP 28	SMC	01 24 11.85	−74 02 32.20	5.29	IM07	3.37	IM07				
MGPN 13	SMC	01 43 10.33	−72 57 03.20	5.53	IM07	3.37	IM07			VS04	
SMP 25	SMC	05 30 33.22	−70 44 38.40	4.87	VS04	4.26	VS04	Broad Hα emission	SH03	SH03	

[25] Possible HII region. The nebula is most likely excited by an eclipsing binary. System of O V type stars.
[26] X-ray source (W91).

Appendix B: Acronyms and bibliographical references

BK13 Balick et al. (2013)
BV97 Bianchi et al. (1997)
DF85 Dopita et al. (1985)
DM91 Dopita & Meatheringham (1991b)
DM91b Dopita & Meatheringham (1991a)
DM91c Dopita & Meatheringham (1991c)
DV97 Dopita et al. (1997)
FG18 Fang et al. (2018)
GH24 Gładkowski et al. (2024)
GM07 Gonçalves et al. (2007)
GM22 Galera-Rosillo et al. (2022)
GM14 Gonçalves et al. (2014)
H96 Hamann (1996)
HA00 Hyung et al. (2000)
HB04 Herald & Bianchi (2004)
HG14 Hajduk et al. (2014)
HP03 Hamann et al. (2003)
IM07 Idiart et al. (2007)
IM18 Iłkiewicz et al. (2018)
JA23 Jones et al. (2023)
KG07 Kniazev et al. (2007)
KL12 Kwitter et al. (2012)
LR06 Larsen & Richtler (2006)
MB88 Monk et al. (1988)
MH12 Melekh et al. (2012)
ML05 Magrini et al. (2005)
MM20 Margon et al. (2020b)
MMb20 Margon et al. (2020a)
MM23 Margon et al. (2023)
MN11 Miszalski et al. (2011)
MP04 Magrini et al. (2004)
OK16 Otsuka et al. (2016)
PM04 Peña & Hamann (2004)
PR97 Pena et al. (1997)
PS07 Peña et al. (2007)
SE09 Saviane et al. (2009)
SH03 Stanghellini et al. (2003)
SL09 Stanghellini et al. (2009)
SR23 Soemitro et al. (2023)
SS05 Stanghellini et al. (2005)
TD24 Tosi et al. (2024)
TR24 Taibi et al. (2024)
VS03 Villaver et al. (2003)
VS04 Villaver et al. (2004)
VS07 Villaver et al. (2007)
W91 Wang (1991)
ZG06 Zijlstra et al. (2006)
ZV94 Zijlstra et al. (1994)